REPUBLIC OF TURKEY

UNIVERSITY OF GAZIANTEP

GRADUATE SCHOOL OF

NATURAL & APPLIED SCIENCES

INVESTIGATION OF THERMAL QUENCHING AND FADING CHARACTERISTICS OF Eu DOPED $CaMoO_4$

M.Sc. THESIS

IN

ENGINEERING PHYSICS

BY

FADHIL SHANSHOOL ALHAMADANI

JANUARY 2017

Investigation Of Thermal Quenching And Fading Characteristics Of Eu Doped $CaMoO_4$

M.Sc. Thesis

in

Engineering Physics

University of Gaziantep

Supervisor

Assoc. Prof. Dr. Vural Emir KAFADAR

By

Fadhil Shanshool ALHAMADANI

January 2017

REPUBLIC OF TURKEY
UNIVERSITY OF GAZİANTEP
GRADUATE SCHOOL OF
NATURAL & APPLIED SCIENCES
ENGINEERING PHYSICS DEPARTMENT

Name of the thesis: Investigation of thermal quenching and fading characteristics of Eu doped $CaMoO_4$

Name of the student: Fadhıl Shanshool ALHAMADANI

Exam date: 10.01.2017

Approval of the Graduate School of Natural and Applied Sciences

Prof. Dr. A. Necmeddin YAZICI

Director

I certify that this thesis satisfies all the requirements as a thesis for the degree of Master of Science.

Prof. Dr. Ramazan KOÇ

Head of Department

This is to certify that we have read this thesis and that in our consensus opinion it is fully adequate, in scope and quality, as a thesis for the degree of Master of Science.

Assoc. Prof. Dr. Vural Emir KAFADAR

Supervisor

Examining Committee Members:	Signature
Prof. Dr. A. Necmeddin YAZICI	.....
Assoc. Prof. Dr. Vural E. KAFADAR	.....
Assist. Prof. Dr. Necmettin NUR	.....

I hereby declare that all information in this document has been obtained and presented in accordance with academic rules and ethical conduct. I also declare that, as required by these rules and conduct, I have fully cited and referenced all material and results that are not original to this work.

Fadhil Shanshool ALHAMADANI

ABSTRACT

INVESTIGATION OF THERMAL QUENCHING AND FADING CHARACTERISTICS OF EU DOPED $CaMoO_4$

ALHAMADANI Fadhil Shanshool

M.Sc. in Physics Engineering

Supervisor: Assoc. Prof. Dr. Vural E. KAFADAR

January 2017, 62 Pages

In this thesis, the heating rate effect on the dose response and TL glow curves of $CaMoO_4:Eu^{+3}$ have been investigated by using the supralinearity function, f(D). The dose response functions have been evaluated using the total areas at different heating rates between 1 $^oC.s^{-1}$ and 10 $^oC.s^{-1}$. The results of this work have showed that, the curves have linear *(f(D)=1)* behavior at very low doses then they are supralinear *(f(D)>1)* up to nearly 10^2 Gy, after this dose level the peaks saturate and go into sublinear *(f(D)<1)* region the heating rates of 1 $^oC.s^{-1}$, 2 $^oC.s^{-1}$, 3 $^oC.s^{-1}$, 5 $^oC.s^{-1}$, 6 $^oC.s^{-1}$ and 10 $^oC.s^{-1}$. But the curves show very different behavior at heating rates of 4 $^oC.s^{-1}$. They show linear *(f(D)=1)* behavior nearly up to 100 Gy, and after this dose level the peaks suddenly saturates and goes into sublinear *(f(D)<1)* region. Also the temperatures of all peaks are shifted higher temperatures and the integrated peak area of the curves decreases by about 15 % as the heating rate increases as expected in theory because of the thermal quenching effect.

Keywords: $CaMoO_4$, heating rate**,** f(D)

ÖZET

Eu katkılı $CaMoO_4$ 'ın termal sönüm ve sönüm karakterisitğinin incelenmesi

ALHAMADANI Fadhil Shanshool

Yüksek Lisans, Fizik Mühendisliği

Tez Yürütücüsü: Assoc. Prof. Dr. Vural E. KAFADAR

Ocak 2017, 62 Sayfa

Bu çalışmada, ısıtma hızının $CaMoO_4:Eu^{+3}$ fosforunun ışıma eğrileri üzerine etkisi doz-cevap fonksiyonu ve doğrusallık fonksiyonu f(D)kullanılarak araştırılmıştır. Doz-cevap fonksiyonu, 1 $^oC.s^{-1}$ and 10 $^oC.s^{-1}$ arasında lineer ısıtma hızları kullanılarak elde edilmiştir. Toplam alan kullanılarak elde edilen f(D) fonksiyonu ısıtma hızları 1 $^oC.s^{-1}$, 2 $^oC.s^{-1}$, 3 $^oC.s^{-1}$, 5 $^oC.s^{-1}$, 6 $^oC.s^{-1}$ and 10 $^oC.s^{-1}$ için düşük dozlarda doğrusal *(f(D)=1)*, 10^2 Gy'e kadar supraliner *(f(D)>1)* ve bu doz değerinden sonra doyuma ulaşarak subliner *(f(D)<1)* özellik gösterdiği fakat ısıtma hızı 4 $^oC.s^{-1}$ için 100 Gy'e kadar doğrusal *(f(D)=1)* bu doz değerinden sonra subliner *(f(D)<1)* özellik gösterdiği gözlenmiştir. Ayrıca ısıtma hızının artmasıyla toplam eğri alanı %15 oranında azalmıştır ve bu azalma teoride belirtildiği gibi termal sönümleme ile açıklanmıştır.

Anahtar Kelimeler: $CaMoO_4$, ısıtna hızı, f(D)

To the spirit of Mom and Dad, my brothers, my wife, my children and my sisters

ACKNOWLEDGEMENTS

I would like to express my deep gratitude to my supervisor Prof. Dr.Vural Emir KAFADAR his guidance, for the continuous support of my M.Sc. study and research, for his patience, motivation, criticism, encouragements and insight throughout the writing of this research work.

My thanks to my professors honored in Physical Engineering Department at everything they gave me.

I also want to warmly thank all my brothers, my sisters and my friends those who have helped me in one way or another. My special thanks are reserved for my family (My Wife, My children DUR, FADAK and ABDULLA). They have given me an endless enthusiasm and encouragement.

I warmly thank Assoc. Prof. Dr. Fatih Mehmet Emen from Mehmet Akif Ersoy University for the synthesis of the sample.

Also, I would like to apologize to all caused them trouble in the Turkish Republic or in my country, Iraq.

Finally, I would like to thank to those who took part in completion of this thesis.

TABLE OF CONTENTS

Page

LIST OF FIGURES

Page

CHAPTER 1

INTRODUCTION

Since about 40 years there has been a noticeable activity in the industry of nuclear power , also is not hidden that the growing utilization of radiation in all areas of life, one of the most important of these areas is a nuclear medicine, Therefore it was necessary to harness all the possibilities for detecting radiation and evaluated, and put certain limits radiological doses to humans and the environment, and here comes the importance of thermoluminescence dosimetry (TLD), as the study of materials that are exposed to ionizing radiation and sends light after heated became the basis for the health experts physical approximately 58 years ago. Since that time, it became a role of thermoluminescence dosimetry is very important and necessary to the safety of people who work in the fields of nuclear or radioactive monitoring, as well as necessary to monitor environmental doses. Moreover, that the thermoluminescence dosimetry is very accurate in the detection of radiation, also had the advantage of small size, available, and inexpensive price, if chosen as suitable material, equivalent to tissue, might have been used to detect gamma rays, neutrons slow, X-rays, beta particles, with the use of suitable filters, it can be used to determine the shallow and deep dose, this allows time effective monitoring of typically uninhabited areas. For to assure right results from long deployments in varied exterior and interior environments, However, various aspects of their performance must be examined.

Dosimetry is the measurement of dose which absorbed by matter or tissue from ionizing radiation and is measured with the SI unit system of Sievert (Sv) or gray (Gy); Where 1 Sv and 1 Gy are equal to 1 joule per kilogram. It is worth mentioning that the non-SI units of rem (Roentgen equivalent in man; for tissue) are still heavily used and rad (absorbed radiation dose; for the matter); their conversions are given by 1 Sv=100 rem and 1 Gy=100 rad. A dosimetry enables us indirectly or directly to assessment exposure dose, absorbed or equipollent dose, kerma and related rates of ionizing radiation.

A dosimetry is characterized by its precision and accuracy, energy response, linearity, spatial resolution, dose and dose rate dependence and directional dependence.

It is very definitely that even little doses of ionizing radiation can stimulate cancer. For this reason, personal radiation control, has become much significant in recent years as the number of probable radiation sources is ever rising [1]. Personnel dosimeter is used in places where the people are exposed to radiation. The target of utilizing personal dosimetry is to control on the level of the radiation exposure of the man to avoid damage resulting from it. ICRP determines the safe limits.

To ensure the completion of these measurements are accurate, a TLD substance must have nearly the same to the human tissue. The TLD substances have to take in the equal quantity of radiation dose as the human tissue. Prior exposing the sick person to ionizing radiations for the diagnosis or the handling procedures, assessments can be simultaneous to thermoluminescence dosimetry (TLD). From the information acquired, possible dose control or extra treatments can be implemented. It is impossible to work so by other means except radiation dosimeter. The main variables determining sick person doses involve technical factors, imaging modality and beam time. In addition to these variables, the volume of the sick person is as well a certain factor. The dosimetry in medicine has two categories; radiotherapy and diagnostics.

There are also some utilizations such as waste disposals, nuclear stations, processing or utilization of disastrous nuclear power plant malfunctions and nuclear fuels introduces elevated levels of radiation and distributes it in the environment. Wherefore, it's become needful to monitor the radiation that transferring to the environment continuously. The (TLD) are utilized for environmental dosimetry applications. It is worth mentioning, the labor standards for (TLD) in this application are contrary to what is in the personnel monitoring. (TLD) must remain has very high sensitivity for long periods, and here is not a requirement to be tissue equivalent.

Accordingly, the (TLD) substance must be stable and intact in the structure in the long interval. In the past few years, Space flight became possible. Types of radiation are present in space and there is no atmosphere to keep the astronauts from radiation, so it is significant to measure the radiation levels at these flights. Furthermore, the high levels of radiation are hurtful for the digital tools of the Spacecraft. For the above

reasons, we need to use the TLD and also can be used TLD in determining processes the age of materials. Renowned researcher, Daniels [2] and some his coworkers were the first to indicate the utilizing of thermoluminescence for this object. All the sections of industry, science and medicine, which utilized ionizing radiation, need to accurate dosimetric tools for radiation levels monitoring. Environmental and personnel dose measurements, both functions are better applianceed utilizing thermoluminescence dosimeters (TLD). The TLD must have the following properties:

- ✓ High sensing to radiation.
- ✓ The influences of non-radiation on the dose storage and readout are low.
- ✓ The dependence on the radiation dose rate is low in (TL) output.
- ✓ Broad range of measuring (from 6 Sv to 105 Sv).
- ✓ (TL) keeps the stocked informations without losses for long period (years).
- ✓ Good stability for radiation.
- ✓ Chemical and Thermal stabilization.
- ✓ Possibility to determine the appropriate TLD for a specific task.
- ✓ Small volume.
- ✓ Low manufacturer cost.
- ✓ It enables us to selectivity in measuring radiation doses.

Most of physical researchers in this field are defined Thermoluminescence as the release of light when some solid materials heated to certain temperature below that of incandescence, this process gets as a result of the presence of defects in crystals ,all crystals contain defects, which may lead to the occurrence of a vacancy in one of the lattice points.

Numerous various synthetic inorganic compounds and natural metals appear the phenomenon of thermoluminescence, but, only a slight section of them provide the requirements mentioned above for thermoluminescence dosimetry. One of important points that should be well in the design of materials luminescence is the mechanism used in energy conversion raised to the light output. [3, 4].

Thermoluminescence (TL) can be explained as the releasing of light from an insulator or a semiconductor when it is heated before the absorption of energy of radiation. It is not the light which is emitted spontaneously from a matter when heated.

Thermoluminescence also can be defined as the emission of light triggred thermally after absorbing energy of radiation. The sent out light is registered as the temperature vs. intensity in the format of one or more TL peaks. The phenomenon of thermoluminescence (TL) of minerals was seen empirically as early as 1663. At this date Sir Robert Boyle notify to the Royal Society around "Experiments and Considerations upon Colors with Observations on Diamond That Shines in the Dark" (1663) and how it was interpreted by, upon calefactory a diamond in connect with his body in the dark, he saw a flash. This illustrates the meaning of thermoluminescence. Not only diamonds, however, a great number of metals release light energy upon calefactory. For examples which are known at that time quartz, flint, feldspar and calcite [5].

There are three fundamental factors necessary for the output of thermoluminescence. Firstly, the substance should be a semiconductor or an insulator-metal does not offer luminescence. As a second, the substance must be exposured to type of radiation for some time and stored some energy. Finally, the substance must be heated for the luminescence release. It is a feature of thermoluminescence that, once heated to produce the light emission, the substance cannot be able to release thermoluminescence one more time by simply cooling the pattern and reheating. so as to re- offer luminescence the substance has to be re-irradiation, At this state can be reheating the pattern to produce light emission one more time. The primary principles that dominate the output of thermoluminescence are basically the same as those that dominate all luminescence operation, and in this way thermoluminescence is merely one of a large family of luminescence phenomena [6].

Thermoluminescence (TL) is watched under situation of steadily rising temperature. In the customary TL experiments, the TL substance are re-irradiated at room temperature (RT) and later heated Within range a temperature where the luminescence is luminous till a temperature level at which all the charges have been thermally agitated out of their metastable levels and the luminescence completely fade. If the light emission intensity is drawn as a function of time or temperature the graphs is famous as glow-curve [7]. Thermoluminescence technique is a relative complicated operation since it contains a luminescence center and a trap. The matters such as semiconductors or insulators is radiate by ionizing radiation at room (low)

temperature, electrons are freed from the valence to conduction band. This generates a hole in the valence band. Both kinds of carriers of charge become movable in their particular bands till they recombine in the recombination center or till they are trapped in lattice defects in the crystalline material. These imperfections of lattice play extremely decisive role in the TL operation. The trap trapped electrons may stay for a long interval while the crystals are keep at low temperature or they can be freed due to the suitable energy given to the electrons while the matter is heated. These electrons may transfer in the crystalline matter till they recombine with convenient recombination centers which inclose hole with the emission of light. This operation of light emission by thermal stimulation from a crystalline solid after irradiations is named as “thermally stimulated operation” or simply “thermoluminescence”. This thermally stimulated light inclose information about the trap structure of the thermoluminescence material and its previous exposure to the ionizing radiations [2].

CHAPTER 2

THEORY OF THERMOLUMINESCENCE IN SOLIDS

2.1 Thermoluminescence mechanism

Thermoluminescence (TL) technique is a moderately complex procedure since it contains a trap and a luminescence center .The fundamental thermoluminescence phenomenon is specific in the figure 2.1. As can be note in this figure, the system contains two bands. One of them that is an energy band which is called the conduction band in a solid. Electrons are moving freely in this band and they can product a shown electric current. The second is the outermost energy band that is called valence band that includes electrons while a solid is in the ground case [10]. Because of radiation which is brought to thermoluminesent substance, release electrons from the (VB) and trapped in the levels of energy in the forbidden gap close to the (CB) (electron trap) is take placed. At the same time, when the electrons are released they will leave holes behind which may be trapped at different energy levels which are also inside the forbidden gap, that is called as recombination center or hole trap [10,11]. After that process, the light must be released while these trapped electrons leave the trap and fall in the lower energy level after heating the pattern [2].

Simply, thermoluminescence may be summarized by: (a) alteration the case of the system from stability case to excited case by absorbing of some ionizing radiation energy; (b) the system turns back to the stability case by releasing the energy which is absorbed from radiation like as visible light with the assist of thermal triggering [11]. In this part, these steps and produce of this light emission will be explained:

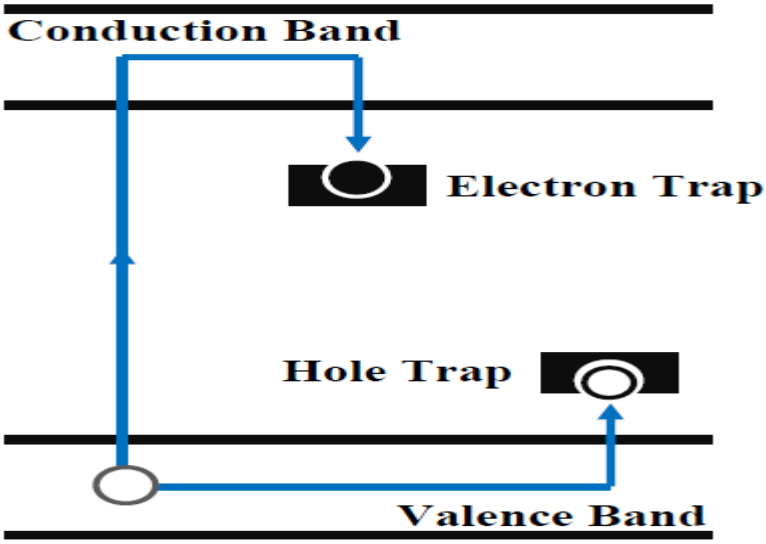

Figure 2.1. Schematic energy level diagram of a phosphor exhibiting thermoluminescence .

2.1.1 Energy Storage

After the sample irradiated, it will absorb some amount of energy, there are two ways to contain that energy, either electronic excitation or damage dislocation. When the sample absorbs the energy of radiation, defects may be created in the crystal structure, these defects are representing states of electronic energy occupied by non-equilibrium concentrations of electrons [13]. Before irradiation, the crystal has localized electronic energy states and after irradiation, some of these states filled by non-equilibrium concentrations of electrons, so, called the defects produced by radiation. McKeever explained that the cause of formation defects is an electronic excitation rather than non-ionizing dislocated damage [11].

Energy storage lead to electronic excitation that happened by the electron-hole pairs. Electron-hole pair production can be defined as the forming of movable holes and electrons in the crystal structure of the pattern after irradiation process. As well as, the mid-gap state, which caused by defects that may be occurred by initial impurities or defects which caused by radiation, which this gap is established between conduction band (CB) and valence band (VB). As to thermoluminescence phenomena it is supposed that there are two types of imperfections named as electron trap and hole trap in the crystal structure which are focused at mid gap cases [2, 11, 14]. At this cases, the electron traps is Located nearby to CB and the hole traps are close from the VB.

Figure 2-2 explains the storage of energy mechanism. After irradiation process, the electrons move from VB to the CB and holes become positively charged region in the valence band. When electron arrives to the CB, it will fall in an electron trap and hole takes its linked trap. A hole trap is named luminescence center in this procedure [2, 11, 14, 15].

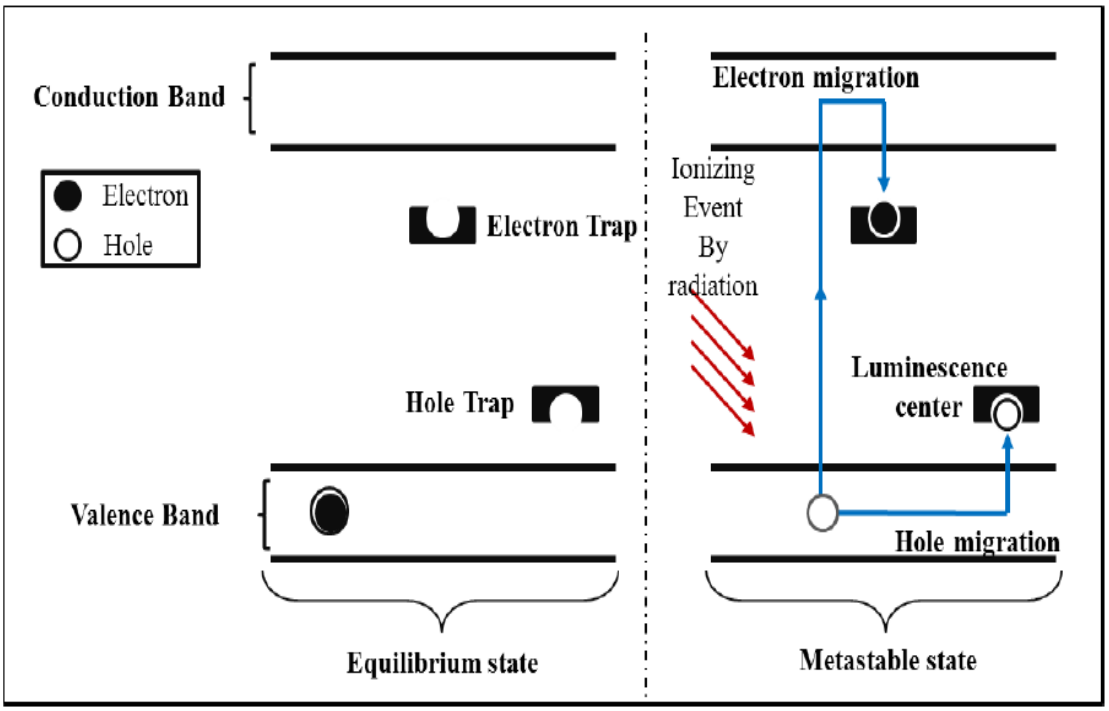

Figure 2.2. Energy storage stage for thermoluminescence operations.

2.1.2 Energy Release

Both kinds of carriers restricted in lattice defects in the crystal. In electron trap electrons stay restricted for a long interval if the crystals are kept at low temperature. When temperature is increased, the electron restricted in the electron trap will move to conduction band, in this case the electron is open to re-trap or recombine with the hole which found in the hole trap. The recombination of the electrons with the holes in holes traps output in the releasing of photons. In this status, hole trap is named as recombination center [2]. This procedure is evident in the figure 2.3.

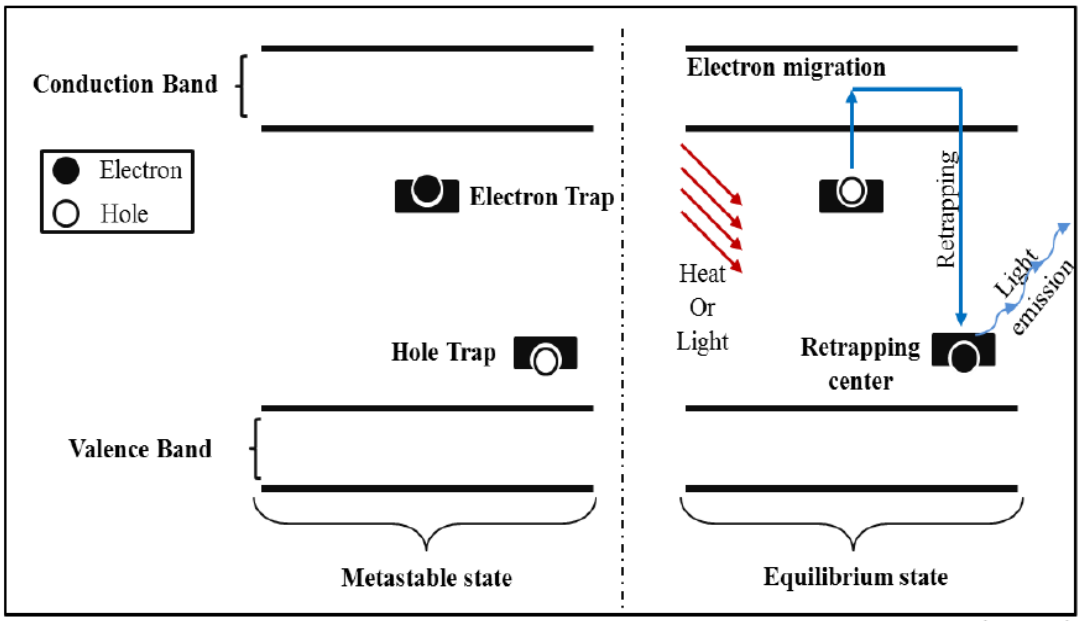

Figure 2.3. Energy release stage for thermoluminescence operations.

2.1.3 Glow Curve

Thermoluminescence signals can be drawn as a curve. This curve is named glow curve that can be understood as a diagram showing of the luminescence intensity as a function of temperature change [2] .In glow curves there is one peak or more of released the light and several of them may be interference with each other. The number of peaks is determined by the host compounds, the species of doped, impurity centers which resulted by radiation, amount of dose and species of ionizing radiation strongly in dosimetric substances [12, 16, 17]. There are several parameters that affect the shape of the curve, like level of dose of the radiation, re-irradiation to elevated doses, thermal handling for the phosphor, and re-handling with specific chemicals. The measure unity of peak intensities in glow curve is an arbitrary unity. Thus, they can be utilized mostly in comparative manner [9 - 11]. Bulk and shape of the glow curves might vary relying on the spectral reply of the light sensitive instrument, various filters utilized amongst the prospector and the pattern. As well as, when the pattern is irradiated it has just single shot influence. The second thermoluminescence releasing cannot be happened by cooling and reheating it. Put that is possible when irradiated sample one more time [2]. Figure 2.4 illustrates several glow curve examples of several thermoluminescent substances.

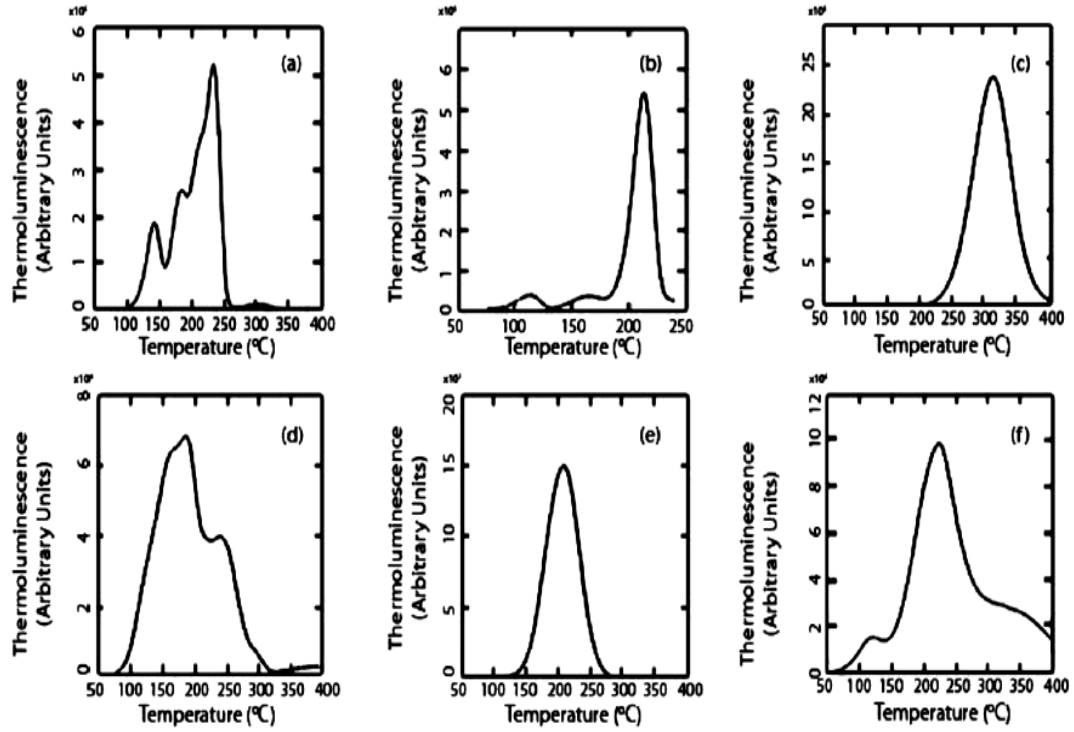

Figure 2.4. Glow curves of some of the main TLD materials, (a) LiF:Mg,Ti; (b) LiF:Mg,Cu,P; (c) CaF_2:Mn; (d) CaF_2:Dy; (e) AI_2O_3:C; (f) $CaSO_4$: Dy [2].

A research of glow peaks leads to information around trapping sites and recombination centers in the structures of crystals, for instance in thermoluminescence dosimetry (TLD), that curve affords information around the radiation dose that the material has been exposed. But generally the major purpose of analyzing and measuring these (TL) glow curves is the detection of various parameters which utilized to characterize the TL procedure in the substance. For instance, the activation energy (E) for the traps (sometimes named the trap depth), the factors of frequency(s), the order of kinetics (b) of the TL procedure, the capture cross-sections for the recombination centers and traps, and their concentrations.

2.2 Simple Thermoluminescence Models

The process by which substances emit light while heated can be comprehend by looking at the easiest possible model composed of two levels, an isolated electron trap (T) and a recombination center (RC), as clear in figure 2.5. This is usually called as the one-trap-one-recombination center model (OTOR).

When symbolized by N to the gross concentration of the traps in the crystal (m^{-3}), by n (t) the concentration of filled traps in the crystal (in m^{-3}). At time t, and by n_h (t)

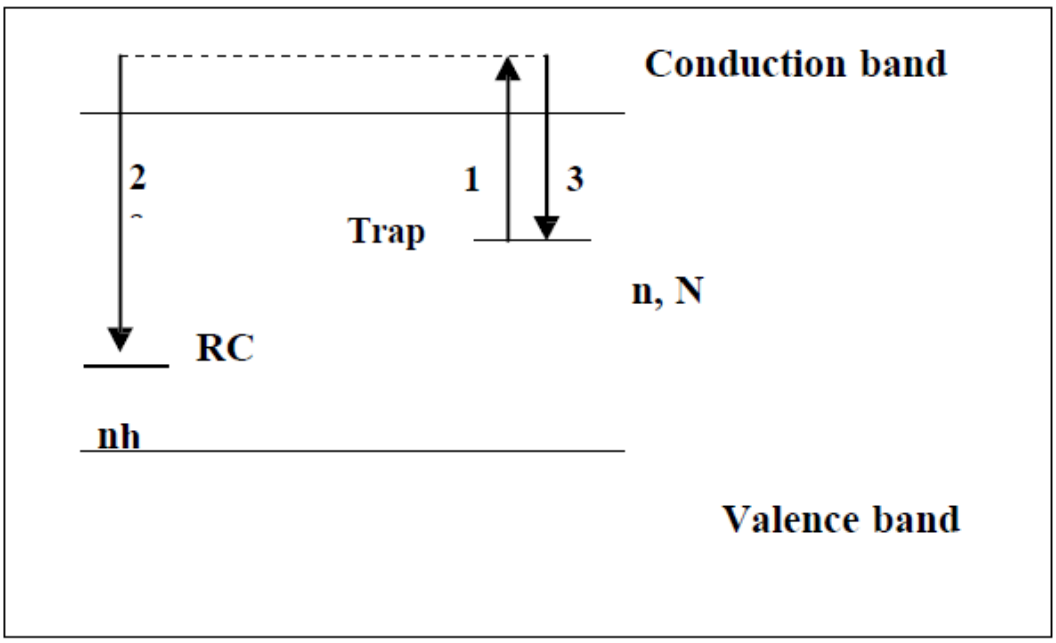

Figure 2.5. Two-level model for the thermoluminescence process [27]

2.2.1 First Order Kinetics

Randall and Wilkins [8, 18] supposed ignored retrapping ((N-n) Ar) through the heating phase i.e. they supposed ($mA_m \gg (N-n)A_n$) and by applying this supposition on the equation:

$$I(t) = \frac{mA_m\, ns\, exp^{\left[-\frac{E}{KT}\right]}}{(N-n)A_n + mA_m} \qquad 2.1$$

$$I(t) = -\frac{dn}{dt} = sn\, exp^{-\frac{E}{KT}} \qquad 2.2$$

The up differential equation portray motion of carriers inside the crystal as a first-order operation, at constant temperature as well probability is constant ($p = exp^{-\frac{E}{KT}}$), and we can define intensity by integrating the equation (2.2).

$$I(t) = I_{\circ}\, exp^{-tp} \tag{2.3}$$

Where ($I_{\circ}$) pointing to the premier intensity at premier time. If temperature variation with time, as well intensity is change and the settling of equation (2.2) becomes:

$$\mathrm{I(t)} = -\frac{dn}{dt} = n_{\circ} s\, exp^{-\frac{E}{KT_{(t)}}}\; exp^{\left\{-s\int_0^t exp^{\left[-\frac{E}{KT_{(t')}}\right]} dt'\right\}} \tag{2.4}$$

Where $n_{\circ}$ pointing to the gross number of restricted electrons at time t = 0, commonly TL is watched while temperature is elevated as a linear function of time as to:

$$T(t) = T_{\circ} + \beta t \tag{2.5}$$

Where, ($T_{\circ}$) represent the temperature with time (t=0) and (β) pointing to the heating rate which is constant. Also, the intensity as a function of temperature turn into:

$$I(T) = -\frac{1}{\beta}\left(\frac{dn}{dt}\right) = n_{\circ}\,\frac{s}{\beta}\, exp^{\left\{-\frac{E}{KT}\right\}}\, exp^{\left\{-\frac{s}{\beta}\int_{T_{\circ}}^{T} exp^{\left\{-\frac{E}{kT'}\right\}} dT'\right\}} \tag{2.6}$$

Eq. (2.6) is a known (Randall–Wilkins) term in first-order when we have single glow peak, however the integral on the right part in the Eq. (2.6) is not easy in the situation of linear heating. But Chen presented that how the integral can be treated by asymptotic set evaluated [19]. In workable applications it is appropriate for illustration the glow peak in expressions of the parameters which are simple to resolve experimentally, Kitis et al [20] presented that the equation (2.6) can be extremely rightly approximated by:

$$I(T) = I_m\, exp^{\left[1+\frac{E}{KT}\frac{T-T_m}{T_m}-\frac{T^2}{T_m^2}\, exp^{\left(\frac{E}{KT}\frac{T-T_m}{T_m}\right)}\left(1-\frac{2KT}{E}\right)-\frac{2KT_m}{m}\right]} \tag{2.7}$$

The characteristics of Randall–Wilkins equation (2.6) which are appeared in Figure (2.7) [21]. When luminescence happened at first, by growing temperature, intensity as well growing pending amount to the maximum point, after this step intensity reduce

(growing intensity led to rise the recombination between holes and electrons, and depletion of charge carriers take effect to lowering of intensity), So the style of intensity resemble a peak shape.

The variation of intensity I(t) may be spotted in the Figure 1a, ($n_\circ$) alter from ($n_\circ$ =0.25 m^{-3}) to($n_\circ$ =2 m^{-3}) while (E=1 eV, s=1.0×10^{12} s^{-1} and β =1 K/s) are lasting constant. It can be apparent that the maximum temperature (T_m) is stable for all peaks. This is an advantage all of first-order TL curves, to finding maximum temperature it can be (or, somewhat easier), from this condition one gets:

$$\left(\frac{\beta E}{KT_m^2}\right) = s\ exp^{\left\{-\frac{E}{KT_m}\right\}} \qquad 2.8$$

The symbol ($n_\circ$) does not note in upper equation (2.8) it led to that (T_m) is Unsupported of $n_\circ$. But in Figure 2.6a, we see that every point of the curve is commensurate to $n_\circ$, as well it is an essential parameter in usage of dosimetry, and it is simple to know that $n_\circ$ is equivalent to the area beneath the glow peak.

$$\int_0^\infty I(t)dt = -\int_0^\infty \frac{dn}{dt}dt = -\int_{n_\circ}^{n_\infty} dn = n_\circ - n_\infty \qquad 2.9$$

The amount (n_∞) is zero for ($t \to \infty$). The most intensity for a first-order kinetics have derived by [22].

$$I_m = n_\circ \frac{\beta E}{KT_m^2}\ exp^{\left(-\frac{E}{KT_m}exp^{\frac{E}{KT_m}}\right)} E_2\ (x) \qquad 2.10$$

Where $E_2\ (x)$ is the exponential integral of second-order, we can see at this equation the peak height is proportional with heating rate β add to $n_\circ$.

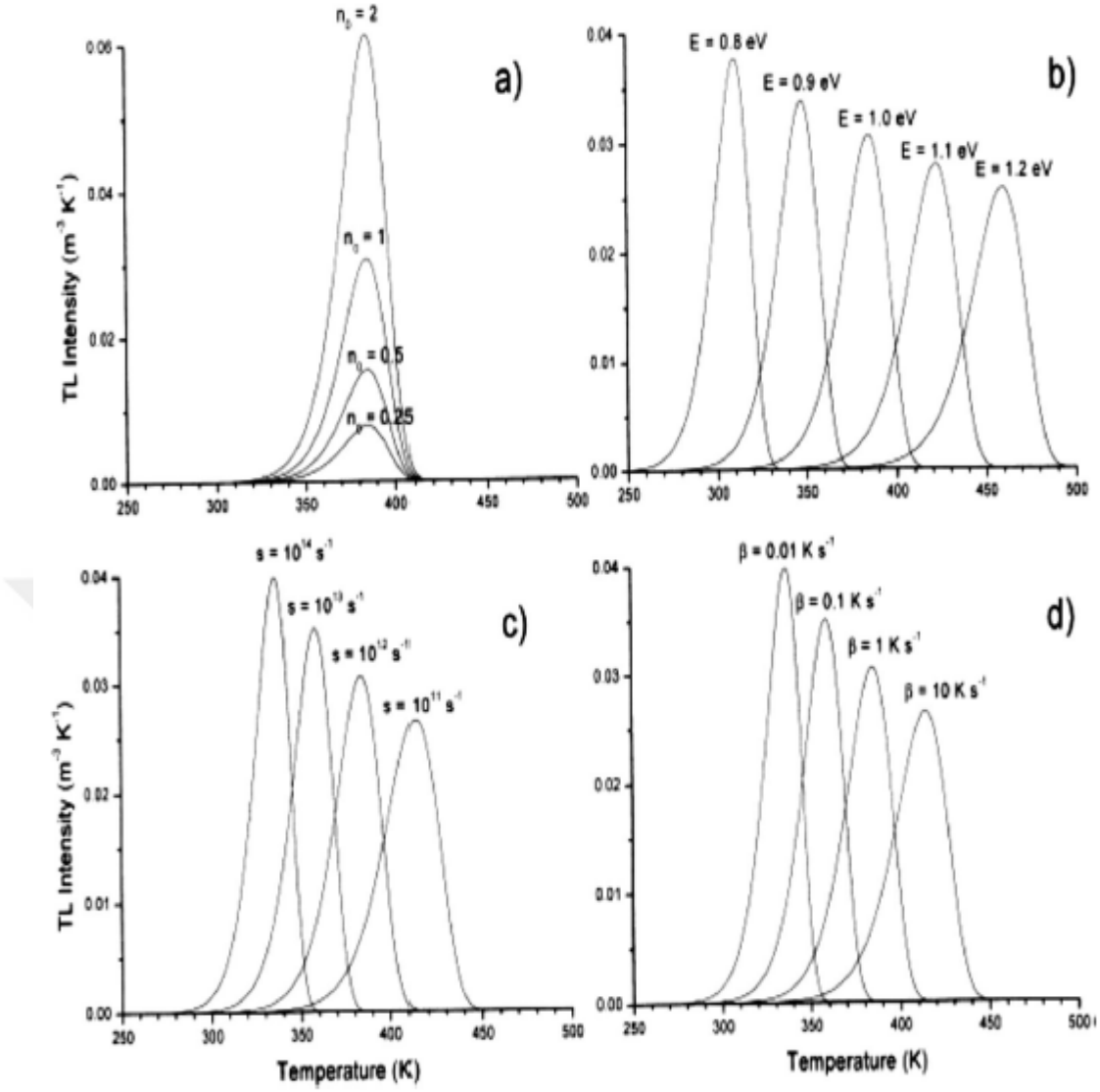

Figure 2.6. Characteristics of the first-order (TL) equation which lay by Randall and Wilkins (a) concentration of the trapped charge carriers after irradiation (n_o), (b) activation energy (depth of trap) (E), (c) the escape frequency (s), and (d) the rate of heating (β). Parameter amounts: (n_o=1 m^{-3}) (E=1 eV) (s=1×10^{12} s^{-1}), of which one parameter is changed whilst the others are stayed constant, and (β =1 K/s) for (a, b, and c) [21].

2.2.2 Second Order Kinetics

The researchers Garlick and Gibson [23] put the second order kinetics to depict a status in which retrapping is existing. ($mA_m \ll (N-n)A_n$). As well they consider that the trap is away from the saturation, i.e. ($N \ll n$) and $n = m$. By these assumptions, the equation (2.2) becomes :

$$I(t) = -\frac{dn}{dt} = s\frac{A_m}{NA_n}\, n^2\, exp^{\left\{-\frac{E}{kT}\right\}} \qquad 2.11$$

When we look at the equation (2.11), it is obvious that the ($\frac{dn}{dt}$) is proportional to (n^2) which means a second-order reaction, and by adding some suppositions, as the eventuality of retrapping and recombination are equal ($A_m = A_n$), if temperature is constant, and after few arithmetic equations the previous equation becomes [21]:

$$I(T) = \frac{n_\circ^2}{N}\,\frac{s}{\beta}\, exp^{\left\{-\frac{E}{KT}\right\}}\left[1 + \frac{n_\circ s}{N\beta}\int_{T_\circ}^{T} exp^{\left\{-\frac{E}{KT'}\right\}} dT'\right]^{-2} \qquad 2.12$$

The previous equation called (Garlick–Gibson) thermoluminescence (TL) equation for the second-order kinetics. We can see in Figure 2.7a, the format of glow curves are roughly uniform, but the section in the end at the right side of the curve in elevated temperature is somewhat wider than the section in low temperature. This expansion in the curve it causes in second-order reaction think that concentrations of freed electrons are retrapped prior they recombine and produce a retard in the release of luminescence and this release is diffusion out over a broader temperature extent. The first concentration ($n_\circ$) is a multiplicative constant in the state of first-order and here furthermore it influenced on the format of curves in various dose levels. And we can view in Figure 2-7a, T_m is vary by changed ($n_\circ$), It can be derived that the temperature variation [24].

$$T_1 - T_2 \approx T_1 T_2 \left(\frac{K}{E}\right) \ln f \qquad 2.13$$

The symbol (T_1) refers to the temperature of the extreme intensity at a given dose and the symbol (T_2) refer to the temperature of the extreme intensity at (f) times higher dose. From the previous Eq (2.13) it follows further that for a given rise of the dose make the trap shallower.

Figures (2.7b, c, and d) depict the distinction in situation and magnitude of a second - order peak as a function of (E), (s/N) and (β) respectively. As in the situation of the first-order kinetics, the area down the curve is proportionate to the premier concentration ($n_\circ$) but there is no longer directly proportional between the peak height and the peak area, in spite of deviation is slight. Despite similarity among both of the second and the first-order to get the trap depth is which can be utilize (initial rise method) that the term bossy the temperature reliance in the premier rise is ($exp^{-E/KT}$). The thermoluminescence (TL) equation of Garlick–Gibson for the second-order kinetics similar first-order kinetics we can write it approximately by expressions of maximum intensity (I_m) and maximum temperature (T_m) [20].

$$I(T) = 4\, I_m exp^{\left[\frac{E}{KT}\frac{T-T_m}{T_m}\right]} \left[\frac{T^2}{T_m^2}\left(1-\frac{2KT}{E}\right) exp^{\left\{\frac{E}{KT}\frac{T-T_m}{T_m}\right\}} + 1 + \frac{2KT_m}{E}\right]^{-2} \qquad 2.14$$

2.2.3 General-Order Kinetics

In previous points (2.2.1, and 2.2.2) the first-order and second-order reaction of the (TL) equation have been concluded by utilizing several simplifying suppositions. However, in fact thermoluminescence peak will not fit the first-order or the second-order kinetics, due to experimentally do not run these simplifying suppositions. Partridge and May [25] utilized a tentative expression in the situation of (general-order kinetics), is:

$$I(t) = -\frac{dn}{dt} = n^b s' exp^{-\frac{E}{KT}} \qquad 2.15$$

Where the (s') is ($m^{3(b-1)}\, s^{-1}$) and (b) is known as the parameter of the general-order and is not needful (1) or (2). Integration of equation (2.14) for ($b \neq 1$) will get:

$$I(T) = \frac{s''}{\beta}\, n_\circ exp^{\left\{-\frac{E}{KT}\right\}} \left[1 + (b-1)\frac{s''}{\beta}\int_{T_\circ}^{T} exp^{\left\{-\frac{E}{KT}\right\}} dT'\right]^{\frac{-b}{b-1}} \qquad 2.16$$

Where the term ($s'' = s' n_\circ^{(b-1)}$) in unit (s^{-1}), Eq (2.15) contains the status of second-order, if (b=2) and modulations to the first-order equation at (b=1), conformity equation (2.15) (s') has a dimension and varied with consideration to the order (b).

Thus in this status can be transact as the first-order at (b→1) and shift to the second-order at (b→2), see the Figure 2.8.

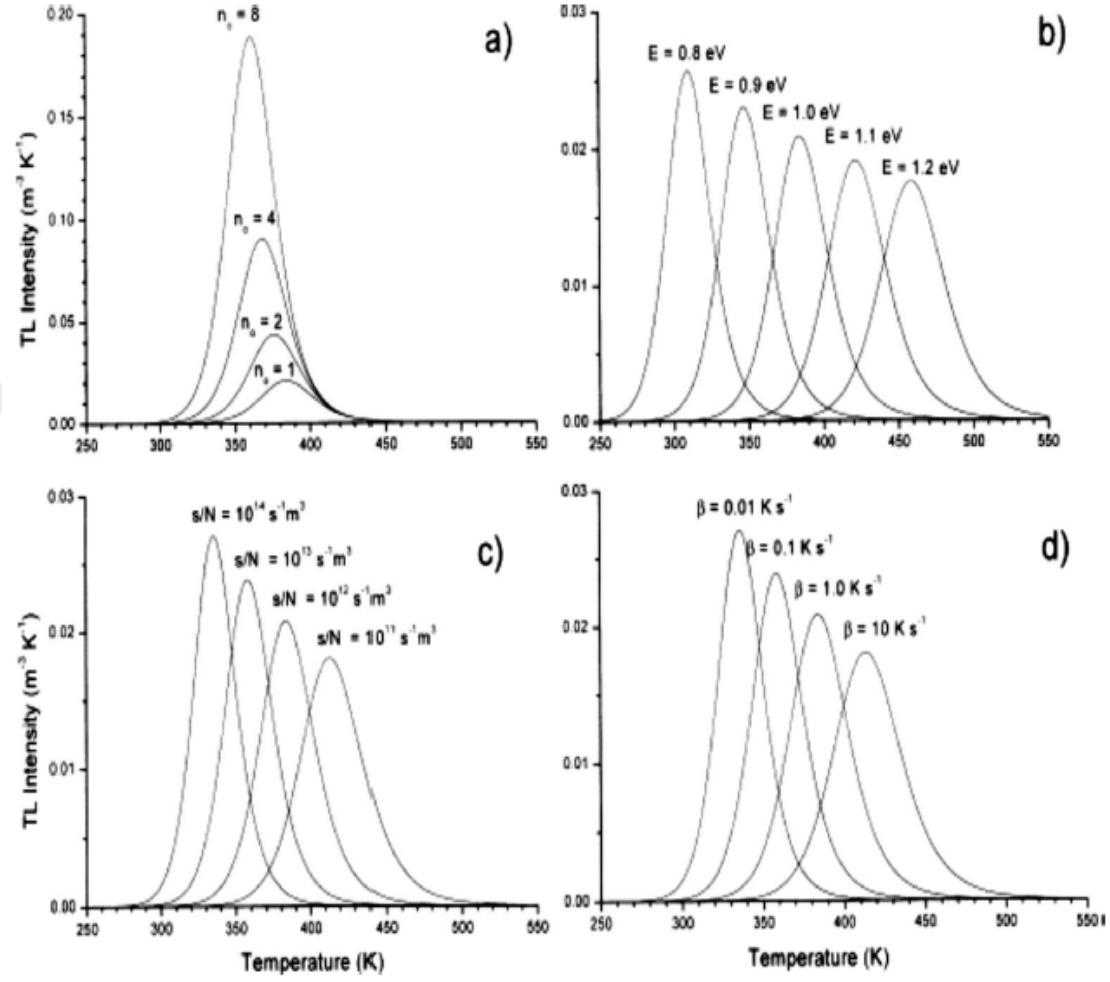

Figure 2.7. Characteristics of Garlick–Gibson second-order TL equation (a) the concentration of trapped charge carrier (n_o) after irradiation; (b) activation energy (E), (c) (s/N), and (d), the heating rate (β). Parameter amounts: (n_o=1 m^{-3}) (E=1eV) (s/N=1×10^{12} s^{-1} m^3), of which one parameter is diverse whilst the others are Stay constant, and (β =1 K/s) for (a, b, and c) [21]

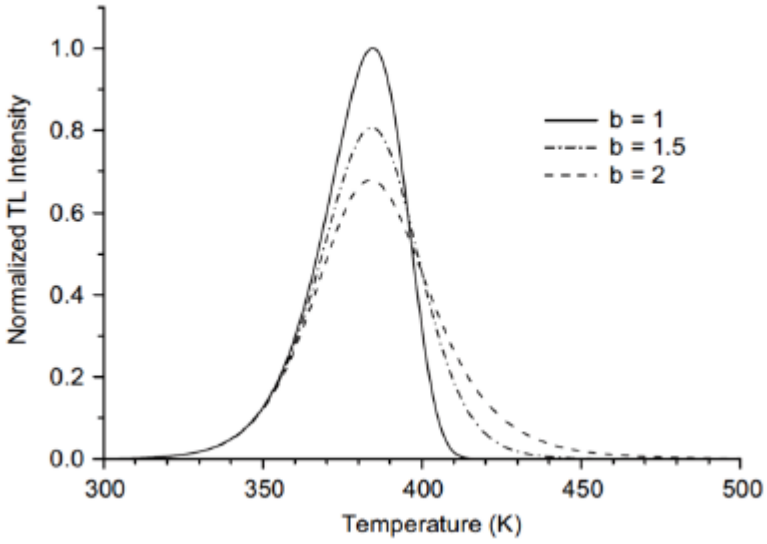

Figure 2.8. Identification of the kinetic orders

The temperature variation appeared as:

$$T_1 - T_2 \approx T_1 T_2 \left(\frac{K(b-1)}{E}\right) \ln f \qquad 2.17$$

The expression (T_1) is the temperature of extreme intensity at a certain dose and (T_2) is the temperature of extreme intensity at (f) times higher dose. And for the general-order equation we can written it by using expressing of (I_m) and (T_m) that has been concluded [26].

CHAPTER 3

THERMOLUMINESCENCE DOSE RESPONSE MODELS

3.1 Overview

In this chapter, we have depicted diverse patterns of modular theory, which characterize the thermoluminescence in a diversity of substances and so existence of large importance in scientific uses of the topic. Likewise, radiation protection and dosimetry that converts the signal TL to a dose of essays instituted on thermoluminescence. And as well we will portray many of the expressions used to portray the nonlinear substance.

The first part of this chapter gives a general review of nonlinear response offered by various substances, and inserts the terminology applied in portraying these nonlinearities. In the second part we will illustrate the competition among traps and thereafter we will portray how to be through irradiation where they can be on the foundation of the existence of a senior number of models composes of kinetic models. In the third part we will illustrate competition through the heating and the excitation stage of TL. Finally, we will explain obtaining the superlinearity index f (D) which will acquaint in the next parts.

3.2 Nonlinear Behaviors of TL Materials

In this part we will provide some essential notions, concerning with experimentally plotted nonlinear behavior of TL substance to radiation. A nonlinear dose response can be described in the following:

$$I_{max} = \alpha S^k \qquad 3.1$$

The term I_{max} acts the extreme TL intensity. S is the values of dose of radiation, α and k are constants.

Halperin and Chen [28] discovered when UV (ultra violet) exposed to irradiated diamonds; its dose response will offer a slope k among 2 and 3 at specific wavelengths. Those authors submitted the expression superlinearity to characterize that more than linear dose response. Chen and McKeever [30] submitted utilizing the expression superlinearity for the growing of the derivative of dose of TL response function. When measurement TL signal is S(D), the growing in the derivative of S(D) is obvious by the truth that the second derivative $d^2 S/dD^2 > 0$. Situations when $d^2S/dD^2 < 0$ are depicted as sublinear, and situations when $d^2S/dD^2 = 0$ are depicted as a linear response. In about low dose domains several TL substances appear linear dose dependence, after that by a superlinear dose domain and by a sublinear domain while close saturation. McKeever and Chen submit utilizing the expression superlinearity to characterize this special nonlinear dose response. Others [31] contained this conduct by inserting the next function called the dose response function f (D) or superlinearity index:

$$f(D) = \left[\frac{S(D)/D}{S(D_1)/D_1}\right] \qquad 3.2$$

The term D_1 refer to normalization dose in the premier linear range. Amounts of f (D) > 1 refer to amounts of S(D) above the premier linear range. In briefly, superlinearity is a measurement of the ratio of change of the dose response for the dose, and superlinearity is characterized quantitatively by the superlinearity index f (D), and is generally utilized in TL uses in dosimetry and dating. Land and Rodine [32] submit that the superlinear behavior of a few substances could be expounded by competition through the heating phase, instead of competition through the excitation step. Kristiapoller et al [29] advanced a formula of thermoluminescence TL patterns of this form. Fogel and Chen [33] research a few of the negatives of these two separate approaches, particularly primary supposition that when the competition happens through the irradiation step, competition is not present through the heating period. Those authors advanced a model that includes the features of the two patterns: competition through heating and excitation models.

3.3 The Filling of Traps in Crystals During Irradiation

The model contains of one trapping status and one center of recombination through irradiation is clear in Figure 3.1. The figure illustrates the allowed hole and electron transitions from the CB and the VB. The trap is recognized by full concentration (N) in the lattice and by immediate electron occupancy n(t). The center of recombination has immediate hole occupancy $n_h(t)$ and full concentration N_h in the lattice. The functions $n_v(t)$ and $n_c(t)$ represent the instantaneous concentrations of free holes in the valence band and free electrons in the conduction band correspondingly. The equations depicting the rate of variation of the functions n(t), $n_h(t)$, $n_c(t)$, and $n_v(t)$ through the irradiation operation are [31]:

$$\frac{dn}{dt} = n_c(N-n)A \tag{3.3}$$

The above equation (3.3) depicts mathematically the actuality that electrons in the conduction band can be restricted into the electron trap.

$$\frac{dn_c}{dt} = R - n_v(N_h - n_h)A_h \tag{3.4}$$

Eq (3.4) depict the operation by which unrestricted holes in the valence band are formed at a constant rate R through the excitation period, and these holes can as well be restricted from the valence band into the center of recombination as indicated by the expression $-n_v(N_h - n_h)\, A_h$

$$\frac{dn_c}{dt} = n_v(N_h - n_h)A_h - n_c - n_h A_r \tag{3.5}$$

Eq (3.5) illustrate the actuality that the holes concentration in the center of recombination is varied by either restriction of electrons from the conduction band (term-$n_c\, n_h\, A_r$), or by restriction of holes from the valence band (term $n_v\, (N_h - n_h)\, A_h$).

$$\frac{dn_c}{dt} + \frac{dn}{dt} = \frac{dn_h}{dt} + \frac{dn_v}{dt} \tag{3.6}$$

Eq (3.6) depicts the preservation of full charge in the lattice, with the left side of the equation being equal to the total immediate concentration of electrons, and the right side of the equation acting the total concentration of holes in the crystal at any time t. The parameters in the previous equations are as bottom:

A = the coefficient of probability of transition the electrons into the trap ($cm^3\ s^{-1}$).

A_h = the coefficient of probability of trapping the holes from the valence band into the center of recombination ($cm^3\ s^{-1}$).

A_r = the coefficient of probability of recombination for electrons from the conduction band into the center of recombination ($cm^3\ s^{-1}$).

n = instantaneous concentration of electrons in the electron trap at time t (cm^{-3}).

N = full concentration of traps of electron in the crystal (cm^{-3}).

(N − n) = instantaneous concentration of empty main traps available at time t.

n_h = instantaneous concentration of holes in the center of recombination (cm^{-3}).

N_h = full concentration of holes in the crystal (cm^{-3}).

n_c = instantaneous concentration of electrons in the conduction band (cm^{-3}).

n_v = instantaneous concentration of holes in the valence band (cm^{-3})

R = constant rate of production of electron–hole pairs per cm^3 per second ($cm^{-3}\ s^{-1}$).

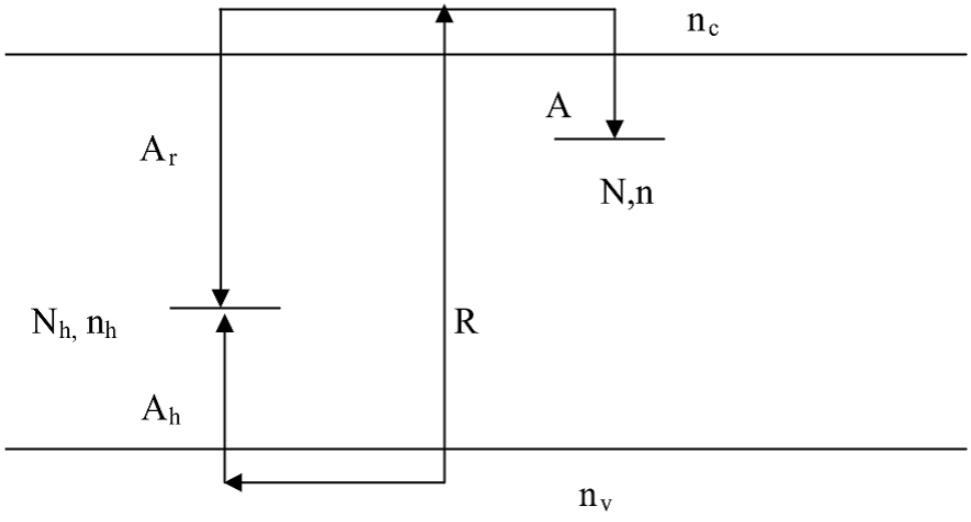

Figure 3.1. The filling of traps during irradiation [5]

3.4 Competition During Excitation Model

This model could explain by utilizing the figure 3.2. There are two trapping states for electrons in this model and it is portray by the full concentrations of electrons N_1 and N_2 and immediate occupancies $n_1(t)$ and $n_2(t)$, respectively [34]. The responsible for TL is the first trap. Trap as the second competitor trap. The form also comprise a center of recombination and the immediate occupancy hole and when our audit operation raised irradiation of electrons in the valence band or in conduction band and be restricted either n_1 and n_2 or with a pair of traps which are competing for electrons as appear in figure 3.2. The kinetic equations for this model are:

$$\frac{dn_1}{dt} = A_1(N_1 - n_1)n_c \qquad 3.7$$

$$\frac{dn_2}{dt} = A_2(N_2 - n_2)n_c \qquad 3.8$$

Equations (3.7) and (3.8) portray mathematically the actuality that electrons in the conduction band can be restricted into either the competitor trap or into the main trap.

$$\frac{dn_c}{dt} = R - \frac{dn_1}{dt} - \frac{dn_2}{dt} - A_k n_c P \qquad 3.9$$

Eq. (3.9) portray the actuality that the electrons in the conduction band are created by the constant excitation rate R, and can be restricted into either of the two traps (terms $-\frac{dn_1}{dt}$ and $-\frac{dn_2}{dt}$) or into the center of recombination (term $-A_k n_c p$).

$$P = n_1 + n_2 + n_c \qquad 3.10$$

The previous equation (3.10) portray the conservation of full charge in the lattice, The left side of the equation being equal to the holes trapped concentration in the center of recombination, The right side of the equation acting the total electrons concentration in the lattice at any instant t. The Eq (3.10) is founded on the supposition that the free holes concentration in the valence band can be obsolete as compared with the accumulated concentration of holes p(t).

The parameters in the previous equations are as below:

A_1 = the coefficient of probability of transition for electrons into the main trap (m^3 s^{-1}).

A_2 = the coefficient of probability of transition for electrons into the competitor trap (m^3 s^{-1}).

A_k = the coefficient of probability of transition for electrons from the conduction band into the center of recombination (m^3 s^{-1}).

n_1 = instantaneous concentration of electrons in the major trap at time t (m^{-3}).

N_1 = full concentration of major traps in the lattice (m^{-3}).

$(N_1 - n_1)$ = instantaneous concentration of empty major traps available at time t.

n_2 = instantaneous concentration of electrons in the competitor trap (m^{-3}).

N_2 = full concentration of competitor traps in the lattice (m^{-3}).

n_c = instantaneous concentration of electrons in the conduction band (m^{-3}).

R = constant rate of generation of electron–hole pairs per m^3 per second ($m^{-3}s^{-1}$).

p = instantaneous concentration of holes in the center of recombination (m^{-3}).

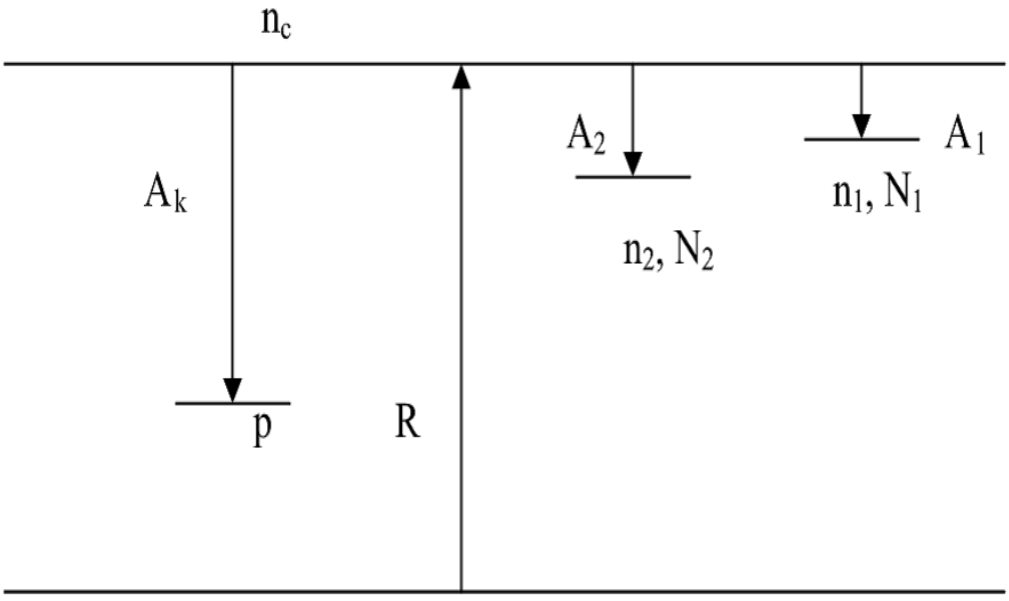

Figure 3.2. The competition during excitation model [27]

3.5 Superlinearity Model with Competition During Both Excitation and Heating

The figures 3.3 and 3.4 illustrate the superlinearity pattern with competition through both heating and excitation [49]. The shape is a two trapping situations and is differentiated by the full concentrations of these electrons N_1 and N_2 and immediate occupancies $n_1(t)$ and $n_2(t)$, respectively. The responsible for TL is the first trap. Trap as the second competitor trap. The pattern also comprises a center of recombination and the immediate occupancy hole and full hole traps concentration given by M.

There are three steps, the irradiation operation it is first, an intermediate relaxation step it is second, and the heating step (measure of TL) is the third. At elevate the irradiation of electrons in the valence band in conduction band and be restricted both n1 and n2 or with a pair of traps which are competing for electrons. These electrons which are in the conduction band may do combine with the holes in the center of recombination at the same period. Through irradiation stage same number of holes are formed in the valence band. Which can be re-trapped at once into the center of recombination growing the hole occupancy m(t).

There are kinetic equations in this pattern for the excitation phase:

$$\frac{dn_1}{dt} = A_1(N_1 - n_1)n_c \qquad 3.11$$

$$\frac{dn_2}{dt} = A_2(N_2 - n_2)n_c \qquad 3.12$$

Eqs (3.11) and (3.12) depicted mathematically the certainty that electrons which present in the conduction band can be restricted into either the competitor or the main trap.

$$\frac{dn_m}{dt} = A_n n_v(M - m)A_m m n_c \qquad 3.13$$

Eq (3.13) depicted the certainty that the quantity of holes in the center of recombination is varied by either restriction extra holes from the valence band (term-$A_n n_v(M-m)$), or by restriction electrons from the conduction band (term $-A_m m n_c$).

$$\frac{dn_v}{dt} = R - A_n n_v (M - m) \quad 3.14$$

Eq (3.14) depicted the certainty that holes are created constantly in the (VB.) valence band by the excitation rate R, but they are also restricted into the center of recombination (term $- A_n n_v(M - m)$).

$$\frac{dn_c}{dt} + \frac{dn_1}{dt} + \frac{dn_2}{dt} = \frac{d_m}{dt} + \frac{dn_c}{dt} \quad 3.15$$

Eq (3.15) depicted the conservation of full charge in the lattice, the left side of the equation being equal to the full rate of variation of the holes concentration, and the right side of the equation being equal to the full rate of variation of the electrons concentration in the lattice.

The parameters in the previous equations are as below:

A_1 = the coefficient of probability of transition for electrons into the main trap (m^3 s^{-1}).

A_2 = the coefficient of probability of transition for electrons into the competitor trap (m^3 s^{-1}).

A_m = the coefficient of probability of transition for electrons from the conduction band into the center of recombination (m^3 s^{-1}).

A_n = the coefficient of probability of capture for holes from the valence band into the center of recombination (m^3 s^{-1}).

n_1 = instantaneous concentration of electrons in the major trap at time t (m^{-3}).

N_1 = full concentration of major traps in the lattice (m^{-3}).

$(N_1 - n_1)$ = instantaneous concentration of empty major traps available at time t.

n_2 = instantaneous concentration of electrons in the competitor trap (m^{-3}).

N_2 = full concentration of competitor traps in the lattice (m^{-3}).

n_c = instantaneous concentration of electrons in the (CB) (m^{-3}).

n_v = instantaneous concentration of holes in the (VB) (m^{-3}).

R = constant rate of generation of electron–hole pairs per m^3 per second (m^{-3} s−1).

m = instantaneous concentration of holes in the center of recombination (m^{-3}).

M = full concentration of holes in the lattice (m^{-3}).

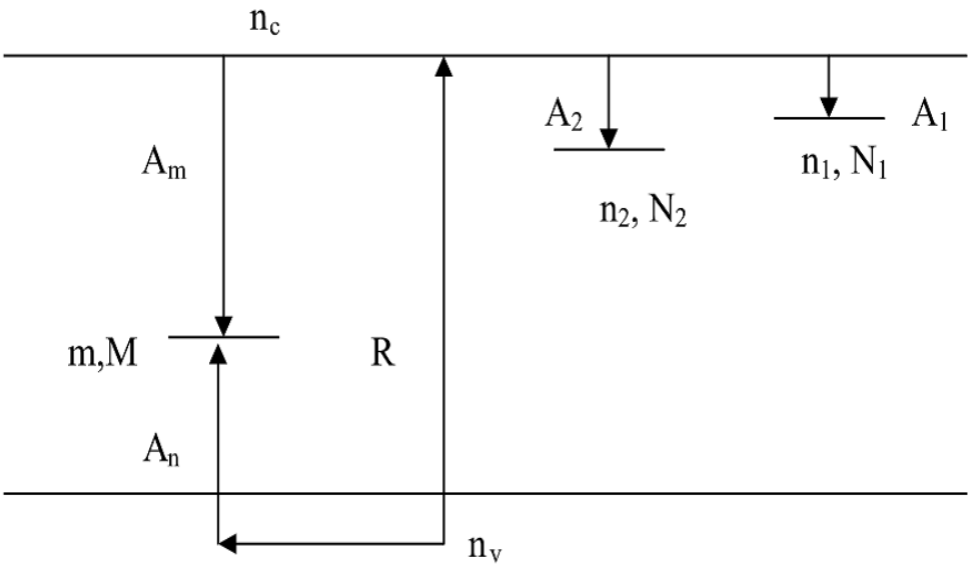

Figure 3.3. Competition during irradiation stage [27]

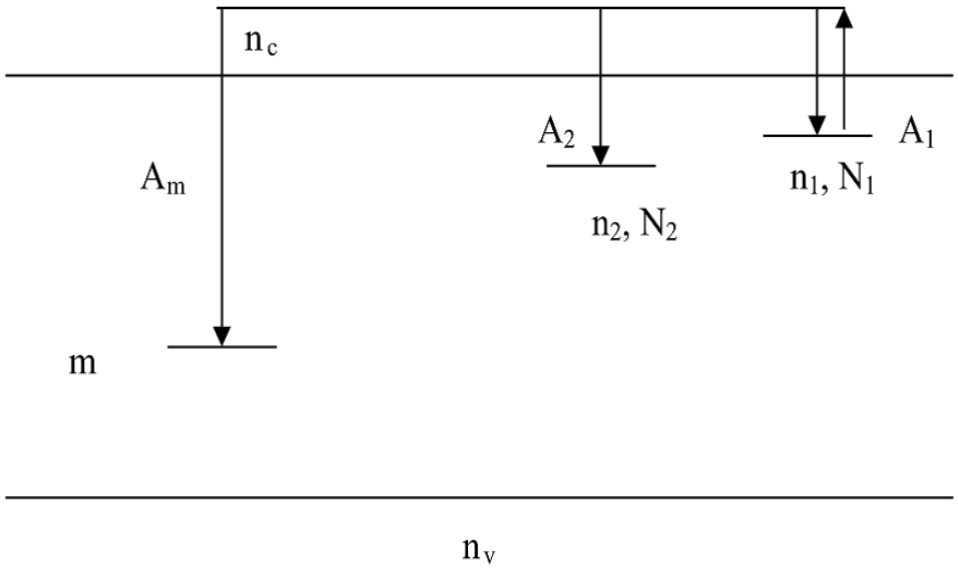

Figure 3.4. Competition during heating stage [27]

3.6 The f(D) Function

Figure 3.5 illustrate the plot y(D) against D gained from the experimental data which have been obtained by the below equation:

$$y(D) = A\left(1 - \exp(-BD)\right) - cD\exp(-BD) \quad 3.16$$

The terms D is the specific dose, A is the TL response at the saturation state (4844 a.u), B = 0.291 × 10^{-2} Gy^{-1}, and C = 12.93 Gy^{-1}.

The superlinearity index f (D) is utilized in the condition where the major target is in the quantity of deviation from linearity, i.e., whether the TL signal is up or down the linear extrapolated field, and to make adjustments if needful [36]. While the superlinearity index f (D) is Known as:

$$f(D) = \left[\frac{S(D)/D}{S(D_1)/D_1}\right] \quad 3.17$$

The next is the significance of the terms that utilized in the last two equations**:**

y refer to the TL signal gained at a particular dose D.

y = y(D) is the analytical term giving the behavior of y as a function of dose D and it is get up by fitting the experimental values.

y′(D) and y′′(D) are, respectively, refer to the first and second derivatives of the function y(D).

D1 is the normalization dose in the premier linear domain of the y = y(D) curve.

In a comparable manner, f (D) < 1 refer to a sublinear felid, f (D) ∼ 0 refer to a saturation felid and f (D) > 1 refer to a superlinearity felid.

The public features in connection with the TL versus dose behavior can be summed up as below:

if y′′ (D) > 0, y′(D) and y(D) increase with D and y(D) is supralinear,

if y′′(D) < 0, y′(D) and y(D) decrease with D and y(D) is sublinear.

if y″(D) = 0, y′(D) is constant with D and y(D) is linear.

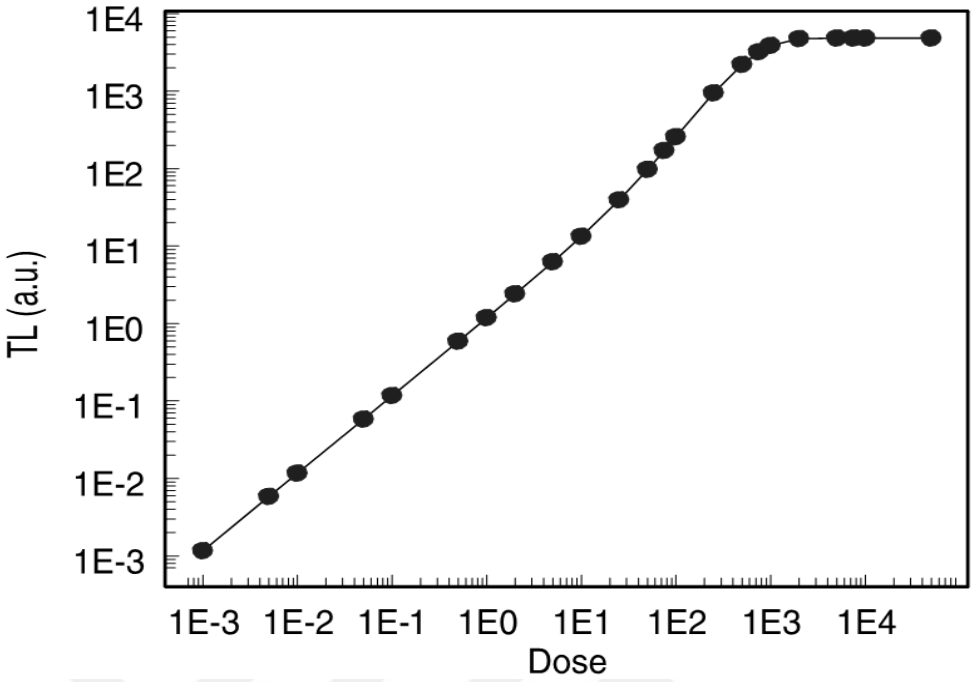

Figure 3.5. TL response versus dose curve [27]

CHAPTER 4

EXPERIMENTAL PROCEDURE AND EQUIPMENTS

The materials, equipments and experimental procedures utilized in this work are described below.

4.1 Experimental Procedure and Equipments

The specimens were irradiated at room temperature by beta particles from a calibrated ^{90}Sr-^{90}Y source. The activity of beta source is around (100 mCi). Stronium–90 emits high - energy beta particles from their daughter products (^{90}Sr β-0.546 MeV together with ^{90}Y β-2.27 MeV). Beta radiation is absorbed by air, so its intensity reduced with distance much more quickly than inverse square law calculations would indicate. The maximum range of Y–90 beta particles in air is approximately 9 meters. The typical strength of a 100 mCi Sr–90 β-source installed in a 9010 Optical Dating System is 2.64 Gy/minute=0.0438 Gy/Sec for fine grains of aluminum, or 3,3 Gy/min=0.055 Gy/sec for 100 m quartz on stainless steel. The equipment of irradiation is an additional part of the 9010 Optical Dating System which is purchased from Little More Scientific Engineering, UK [37].

The irradiated specimens were read out by a reader of Harshaw QS 3500 manual type that is attached to a PC where studied and analyzed. A clear glass filter has been placed in the reader between the photomultiplier tube and planchet to eliminate the emitted infrared lights from the samples plus reader. The device contains a sample change drawer for removing and inserting the TLD elements. For improving the low-exposure reading accuracy and to extend planchet life, the 3500 provides for nitrogen to flow around the planchet. Through the elimination of oxygen in the salinity, flow of nitrogen eliminates unwanted TL signal caused by the oxygen. Nitrogen is also directed through the photo-multiplier tube (PMT) chamber to eliminate moisture caused by condensation.

4.2. Synthesis of Europium doped Calcium Molybdate $CaMoO_4:Eu^{+3}$

The raw materials including MoO_3, $Ca(NO_3)_2$, Eu_2O_3, were purchased from Merck and used as received without further purification. Calcium Molybdate ($CaMoO_4:Eu^{+3}$) have been prepared by the complex polymerization method (CPM). In this synthesis, molybdate citrate was formed by dissolution of MoO_3 and citric acid in aqueous solutions. The citrate solution was well homogenized under constant stirring at a temperature of ~ 60-80°C. After achieving complete dissolution was add stoichiometric amounts of $Ca(NO_3)_2$. The complex was well stirred for several hours at 80–90°C to produce a clear, homogeneous solution. After the solution was homogenized, ethylene glycol was added to promote the polyesterification. With continued heating the viscosity of the solution increased, albeit devoid or any visible phase separation. After partial evaporation of the water, the resin was heat treated at 300°C for 2 h, in a static oxidizing atmosphere, leading to the partial decomposition of the polymeric gel, forming an expanded resin, constituted of partially pyrolyzed material.This pre-pyrolyzed material was removed from the beaker and deagglomerated using mortar.

Figure 4.1 Irradiation part

Figure 4.2 TLD reader

CHAPTER 5

EXPERIMENTAL RESULTS

Metal molybdates ($XMoO_4$, X = Ca, Sr, Ba) have a great potential for application in various fields such as photoluminescence, microwave applications, optical fibers, scintillator materials, humidity sensors, and catalysis. Calcium molybdate ($CaMoO_4$) crystal is important amongst the metal molybdate family, which has a high potential to be applied in cryogenic scintillation detectors and double beta decays. Moreover, it has many interesting physical characteristics such as luminescence, reflectivity and thermal properties. Therefore, synthesis of $CaMoO_4$ crystals has received great attention [37]. $CaMoO_4$ with a scheelite type structure has been of practical interest for a long time because of its attractive luminescence. It provides green emission as an available solid-state laser material. Various techniques, which need high temperature and harsh reaction conditions, have been developed to synthesize $CaMoO_4$, such as the Czochralski method, and coprecipitation, combustion and conventional solid-state reaction. $CaMoO_4$ powders prepared by these processes are relatively large in particle size with irregular morphology, and of inhomogeneous composition due to MoO_3 tendency to vaporize at high temperatures.

To overcome these disadvantages, the citrate complex method has been successfully used to synthesize $CaMoO_4$ nanoparticles, but this method is complex, and involves the use of large amounts of organic solvents, and still needs a relatively high calcination temperature of 600 ^oC [38]. Rare-earth-doped upconversion (UC) materials have ability to convert low energy near infrared (NIR) light to higher energies. UC nanoparticles have attracted the interest in recent years as their promising applications in optical fibers, bioimaging, drug delivery, solar cells and display devices. Currently, rare-earth-doped upconversion nanoparticles can be synthesized by combustion synthesis method, chemical co-precipitation method, sol–gel method, thermal decomposition method and hydrothermal method [39].

Metal molybdates are important inorganic materials which have potential applications in photoluminescence (PL), hosts for lanthanide-activated lasers, photocatalysis, and scintillation detectors. Metal molybdates with large bivalent cations (Ca, Ba, Pb, and Sr) mainly exist in a scheelite-type tetragonal structure, whereas those with small cationic radii (Zn, Fe, Mn, Co, and Ni) generally have a wolframite-type monoclinic structure. Among them, scheelite $CaMoO_4$ have gained much attention due to their high density (4.25 g/cm^3), high irradiation, thermoluminescence, and relatively low phonon threshold energy compared to other oxide materials. This compound exhibits self-luminescence in visible spectrum which could be decomposed in blue, green, and red components. Also, these serve as excellent host materials for trivalent lanthanide ions, which produce spectral emission lines due to f–f transitions [40]. Solid-state lasers operating in the yellow region (570–590 nm) could have important technological applications (military, telecommunication, commercial, etc). However, they have not been realized up to now because of the difficulties in finding materials suitable for this purpose. $CaMoO_4$ belongs to the family of the tungstates and molybdates having general formula MXO_4 (M = Ca, Sr, Ba; X = W, Mo) and scheelite structure. These crystals have been reported to be good host lattices for lasing ions on one hand, and suitable materials for the development of Raman lasers on the other. The absorption (360–1900 nm) and emission (460–850 nm) spectra and the decay curves of the luminescence were measured at temperatures ranging from 10 to 298 K [41].

In this research we have investigated the dose response characteristics of (Eu doped $CaMoO_4$) at different linear heating rates (β) between 1 °C and 10 °C by using the dose response function f(D). Eu doped $CaMoO_4$ was irradiated at room temperature with beta rays from a ^{90}Sr- ^{90}Y source (≈0.04 Gy/s). Heating rate (β) is one of the essential requirements of thermoluminescence dosimeters (TLD) in searching the dosimetric parameters. It was confirmed that the reduction in TL response with increasing heating rate attributed to thermal quenching of luminescence in TLD. In this research the influence of the heating rate (β) on the dose dependence of the essential dosimetric peak and on the overall peak area of the glow curves of Eu doped $CaMoO_4$ have been investigated. Typical glow curves of $CaMoO_4$:Eu sample using a linear heating rate between 1 ^oC and 10 ^oC are shown in Figures 5.1-5.8.

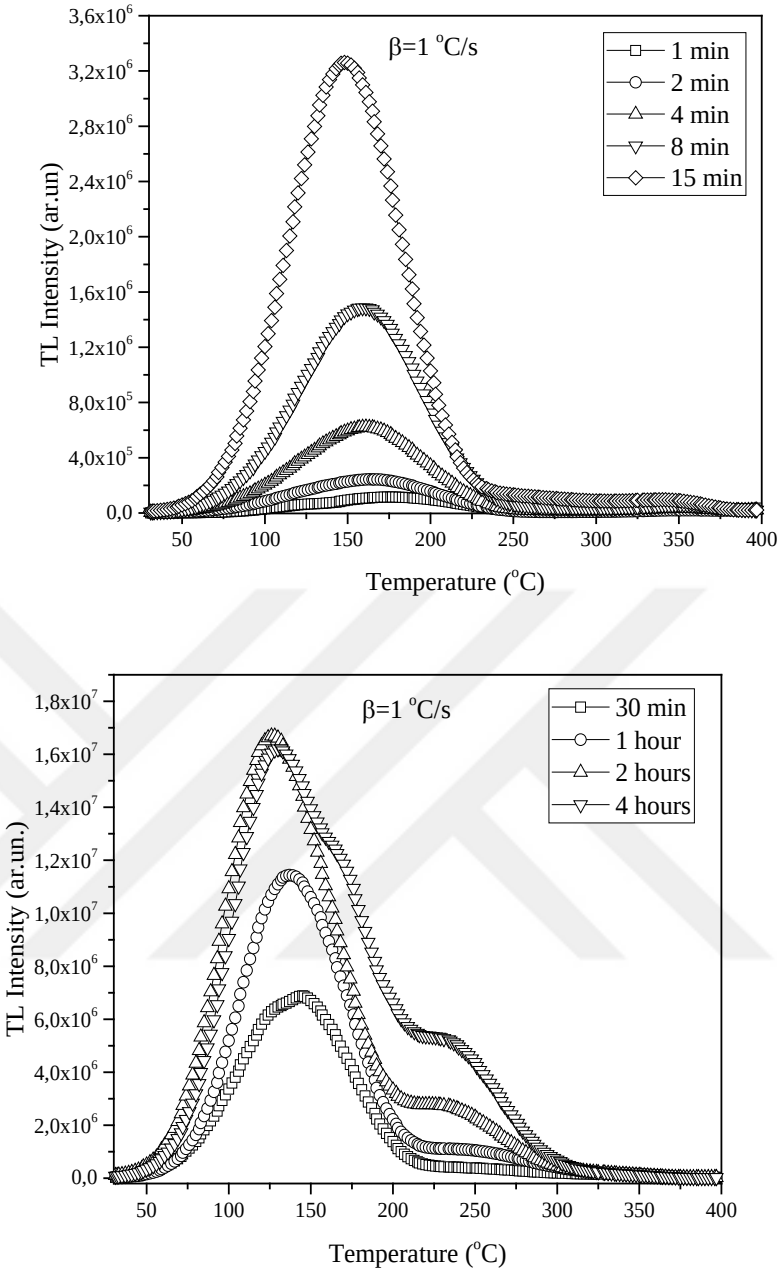

Figure 5.1. Typical glow curves of Eu doped $CaMoO_4$ exposed to β-rays from 2.4 Gy to 576 Gy at $\beta = 1\ ^{o}C.s^{-1}$

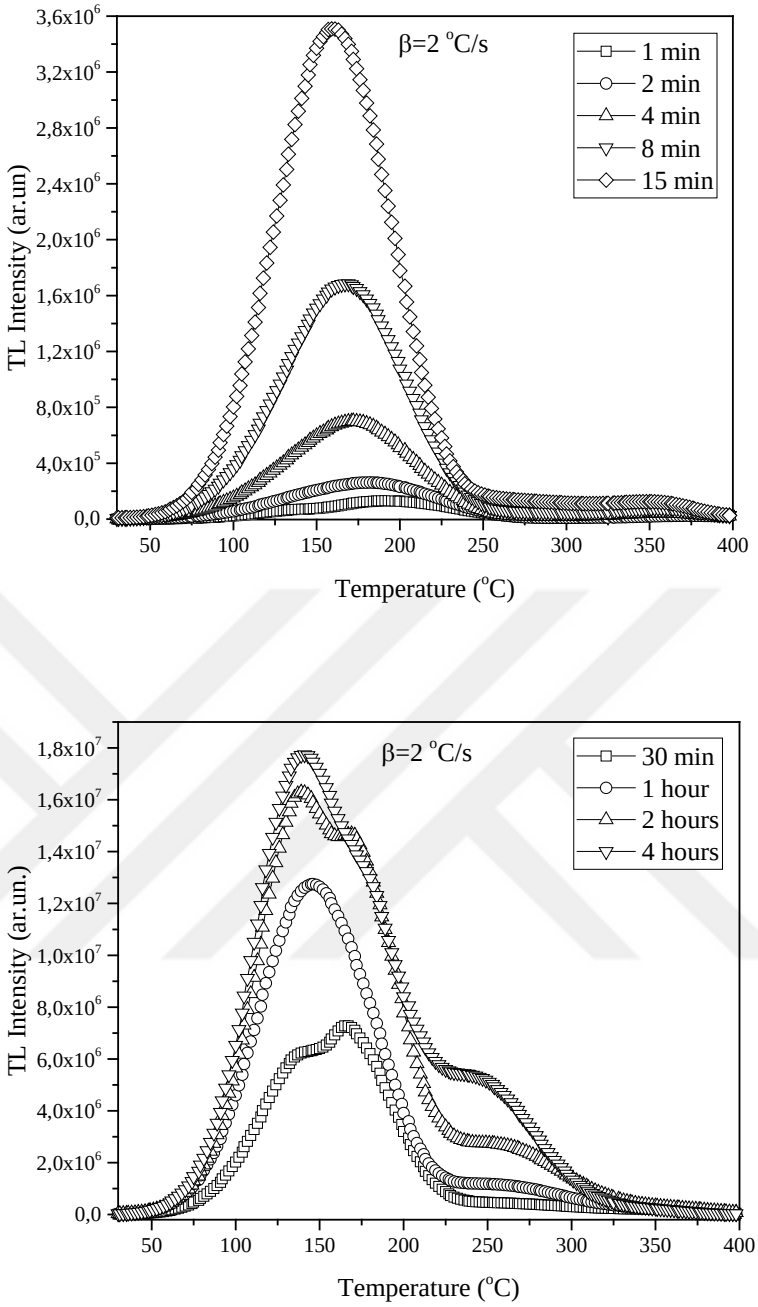

Figure 5.2. Typical glow curves of Eu doped $CaMoO_4$ exposed to β-rays from 2.4 Gy to 576 Gy at $\beta = 2\ ^{o}C.s^{-1}$

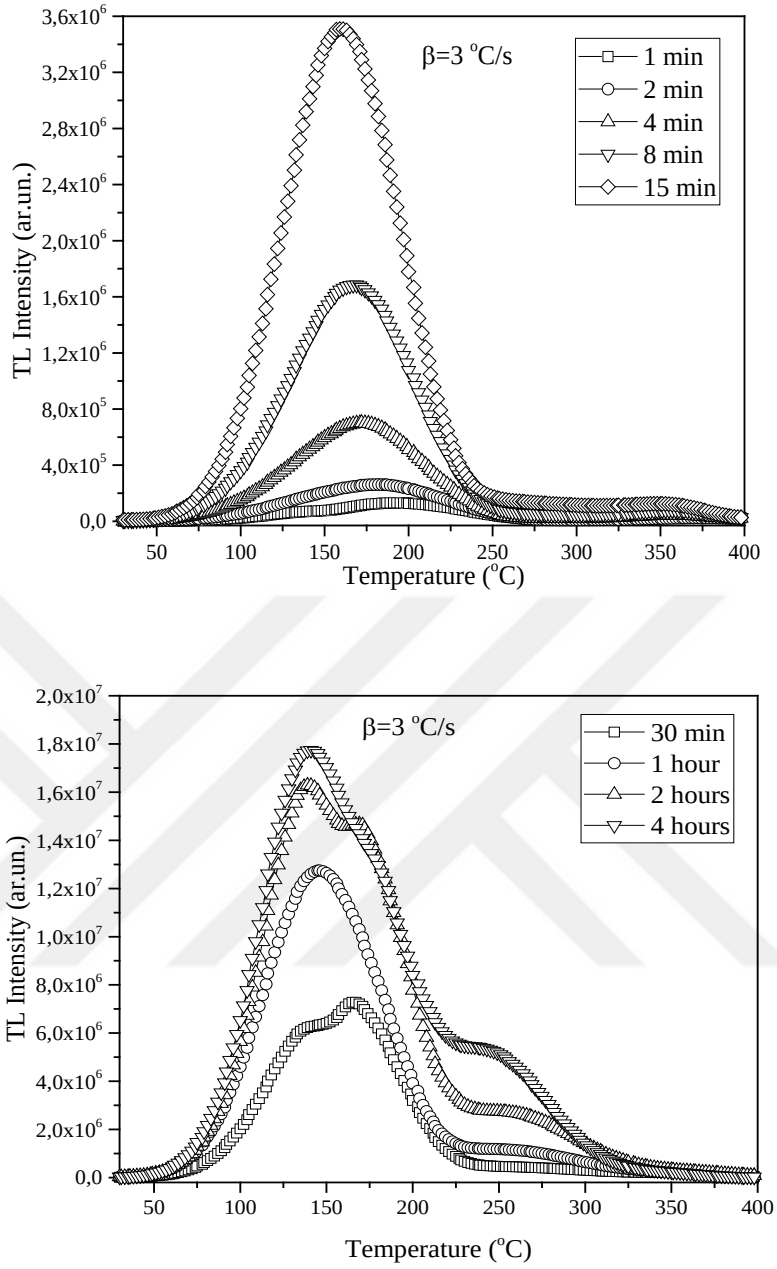

Figure 5. 3. Typical glow curves of Eu doped $CaMoO_4$ exposed to β-rays from 2.4 Gy to 576 Gy at $\beta = 3\ ^{o}C.s^{-1}$

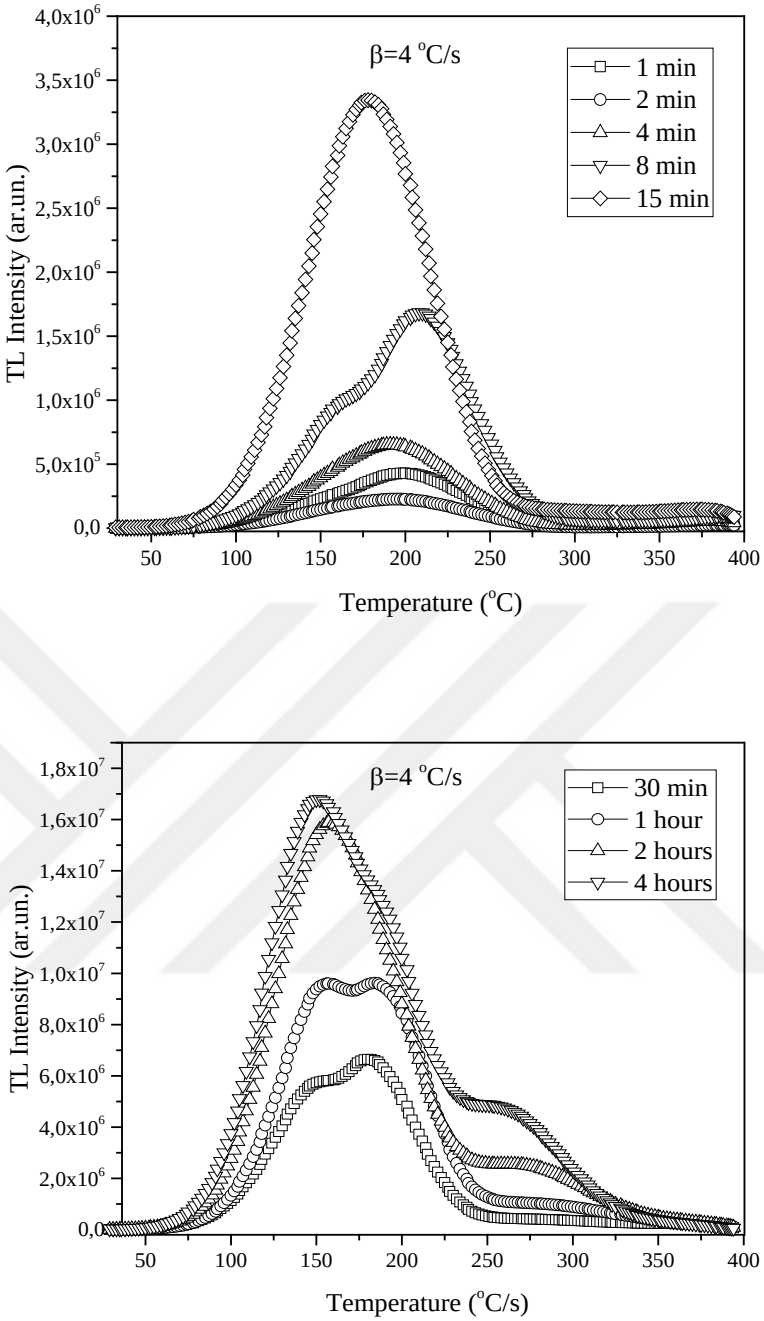

Figure 5. 4. Typical glow curves of Eu doped $CaMoO_4$ exposed to β-rays from 2.4 Gy to 576 Gy at $\beta = 4\ ^{o}C.s^{-1}$

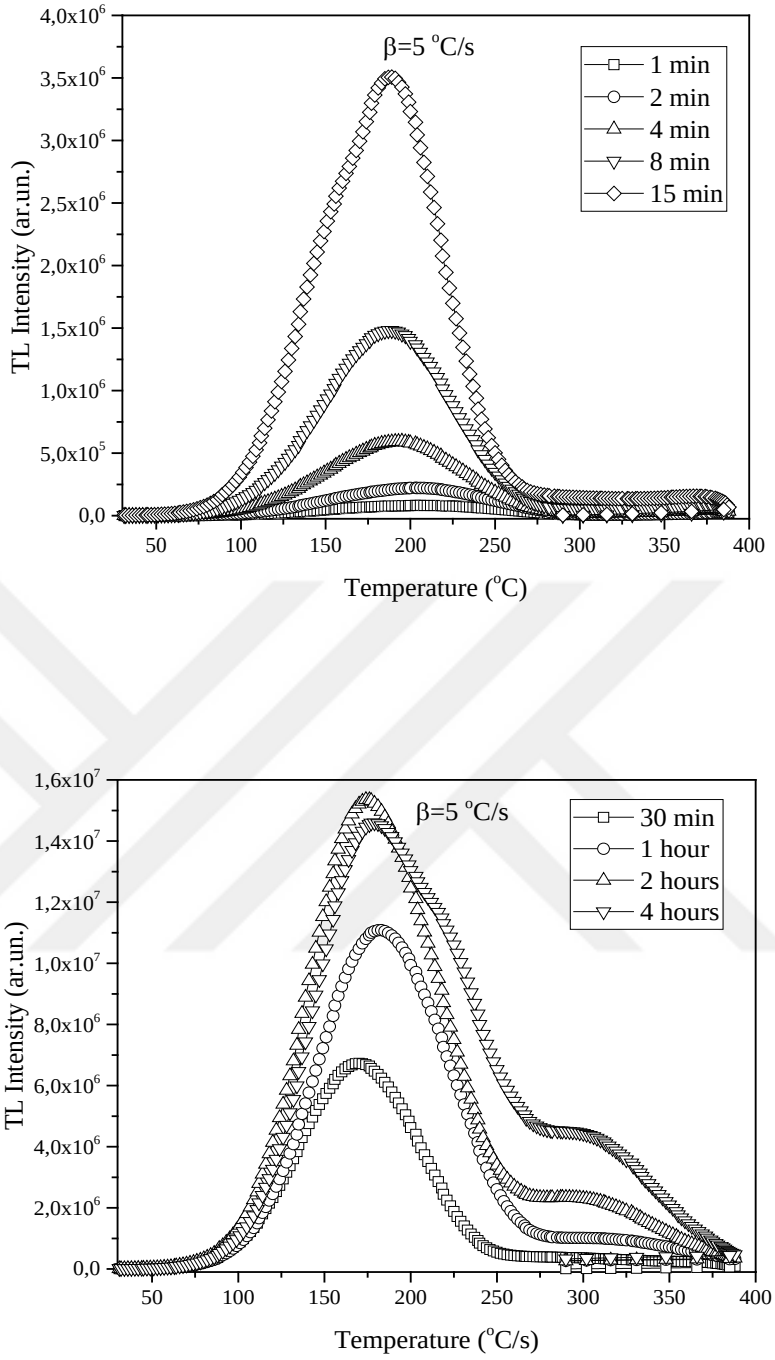

Figure 5.5. Typical glow curves of Eu doped $CaMoO_4$ exposed to β-rays from 2.4 Gy to 576 Gy at $\beta = 5\ ^{o}C.s^{-1}$

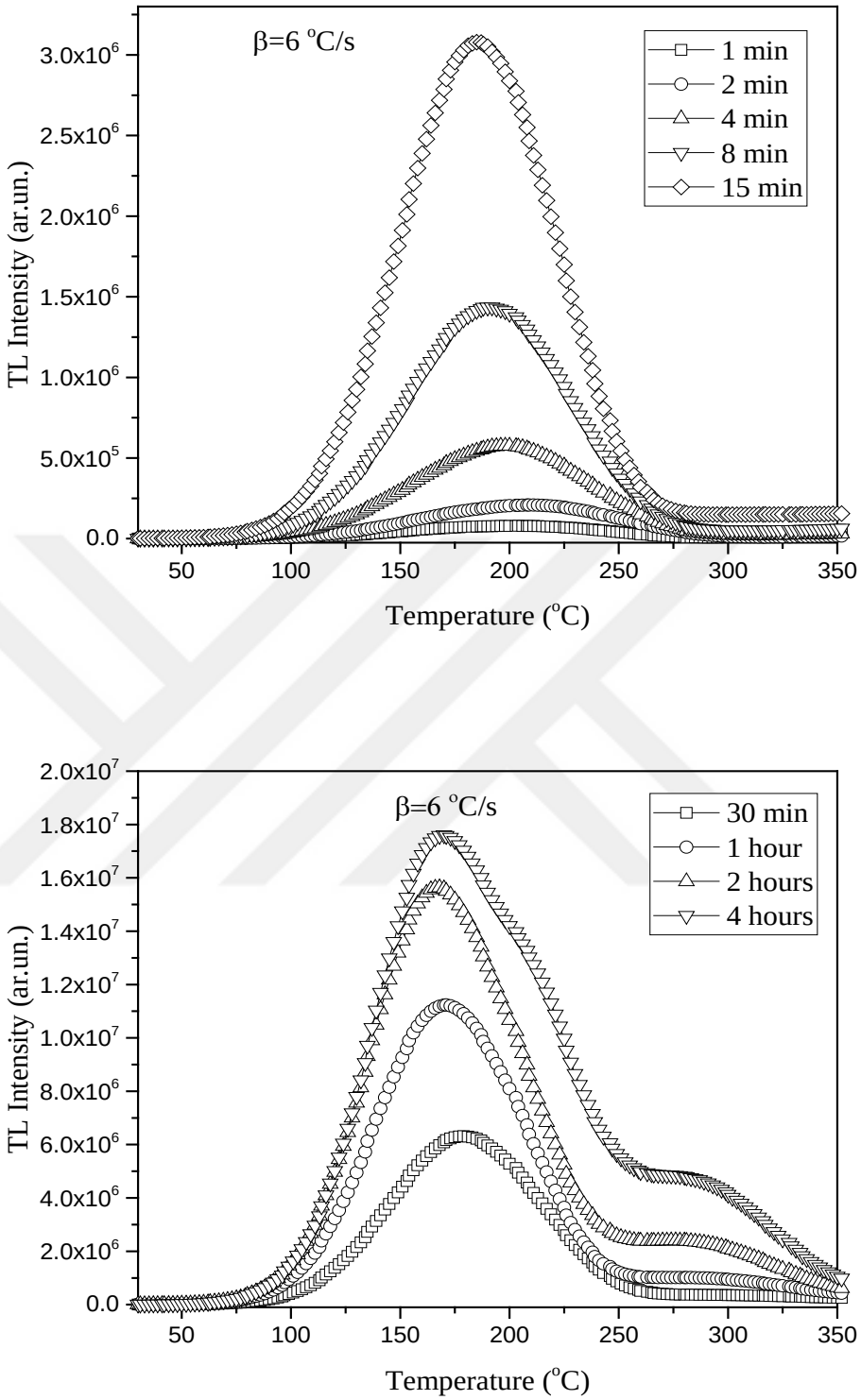

Figure 5.6. Typical glow curves of Eu doped $CaMoO_4$ exposed to β-rays from 2.4 Gy up to 576 Gy and readout at linear heating rates of β = 6 °C.s^{-1}

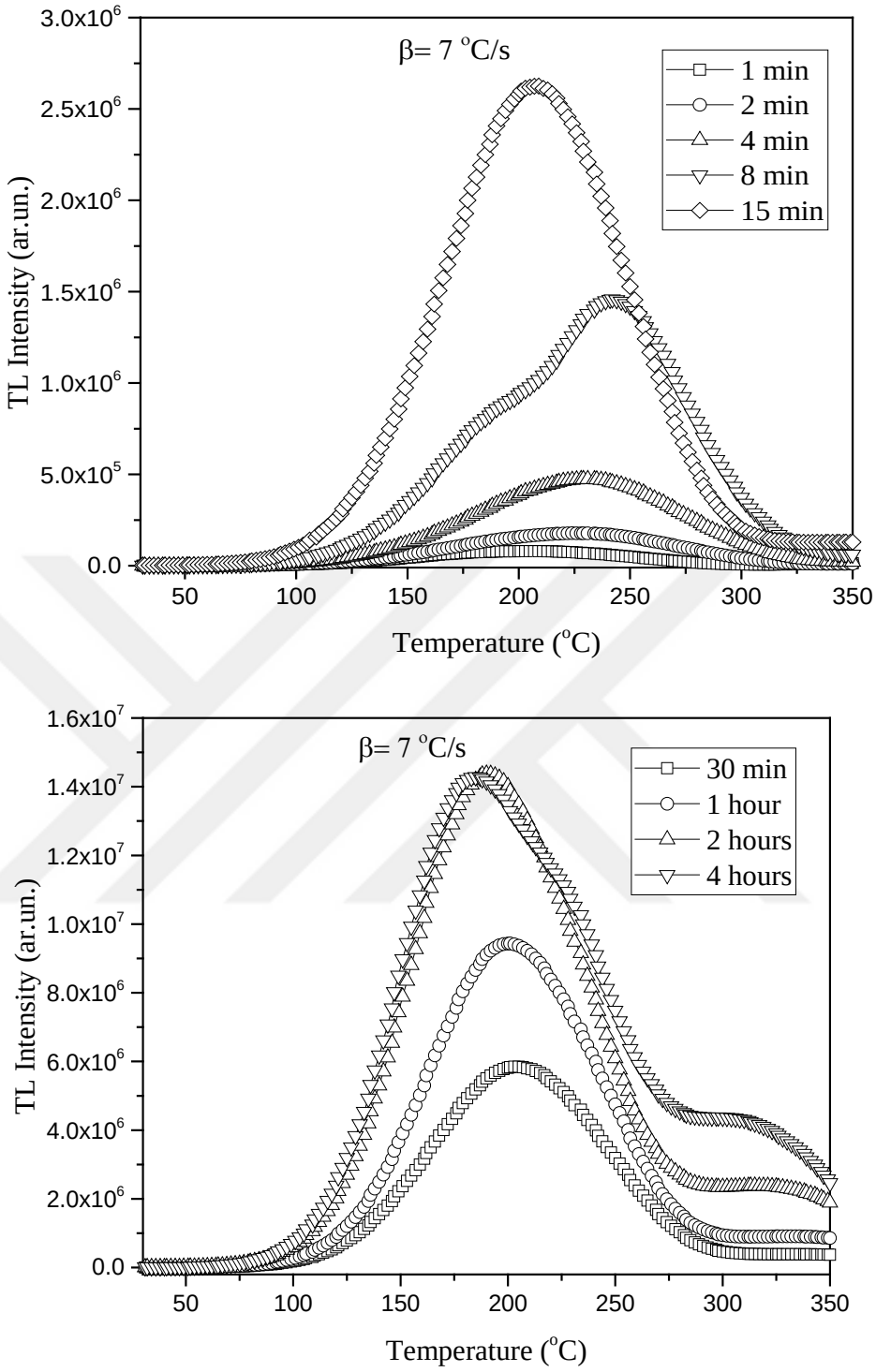

Figure 5. 7. Typical glow curves of Eu doped $CaMoO_4$ exposed to β-rays from 2.4 Gy to 576 Gy at $\beta = 7\ ^{o}C.s^{-1}$

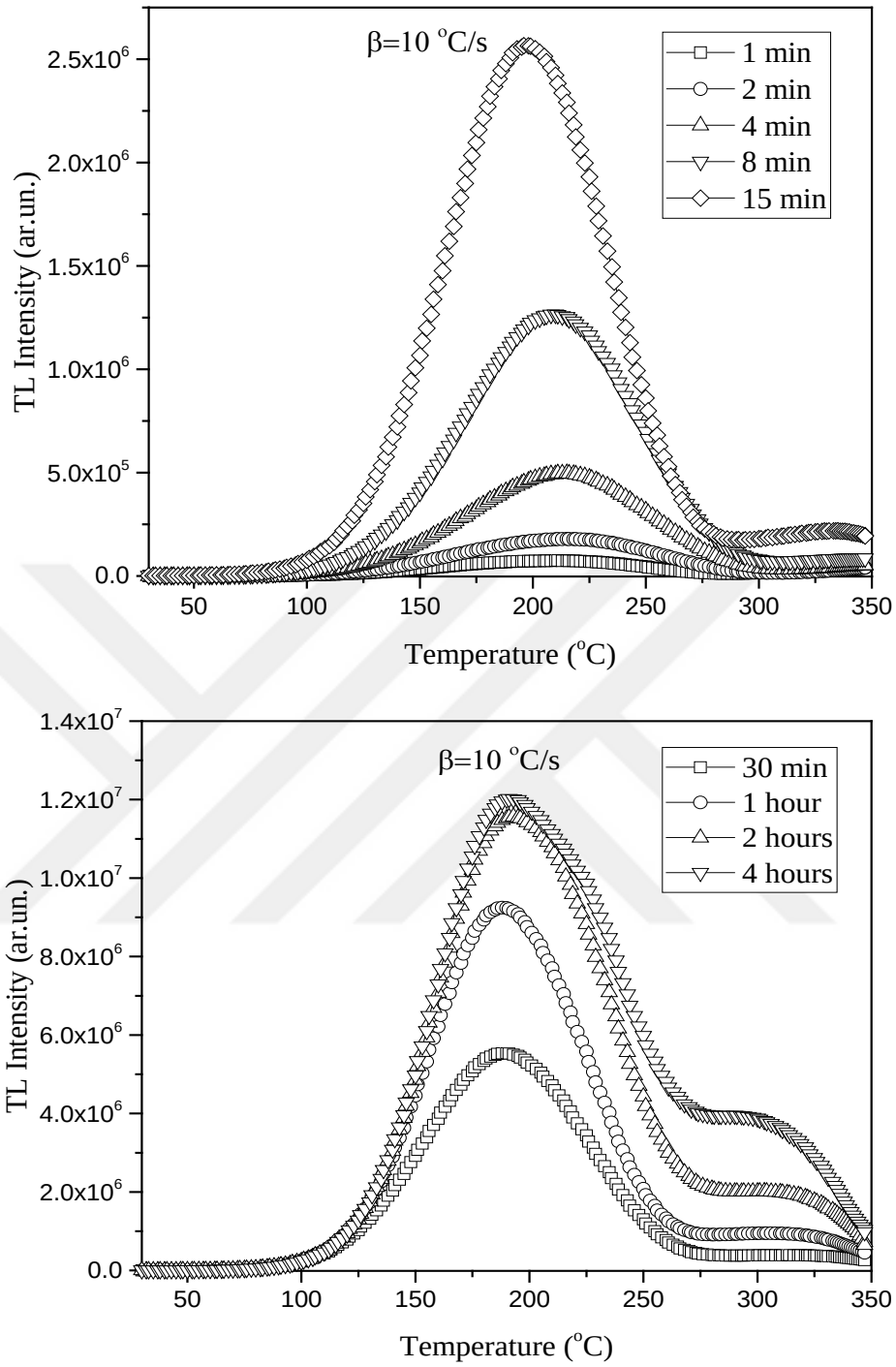

Figure 5. 8. Typical glow curves of Eu doped $CaMoO_4$ exposed to β-rays from 2.4 Gy to 576 Gy at β = 10 $^{o}C.s^{-1}$

Figures 5.9-5.12 show the growth of the height of the peaks as a function of dose. As seen from these figures, the intensity of the main peak of Eu doped $CaMoO_4$ linear behavior up to elevated dose levels particularly at low heating rates (β). But when the

heating rate is increased the peak shows a linear region at low doses. When the dose level is increased the peak goes into the supralinear region after 10^2 Gy then the peak saturates and goes into sublinear region after 10^3 Gy at high heating rates.

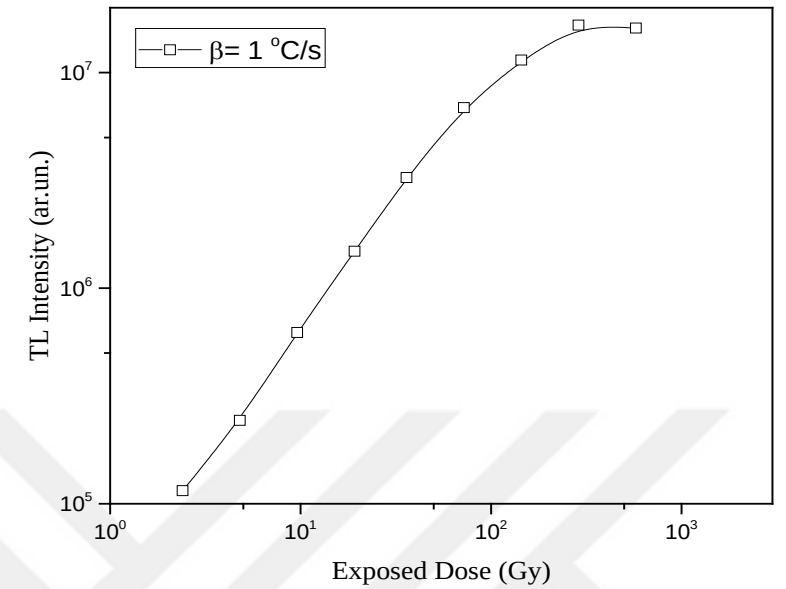

(a)

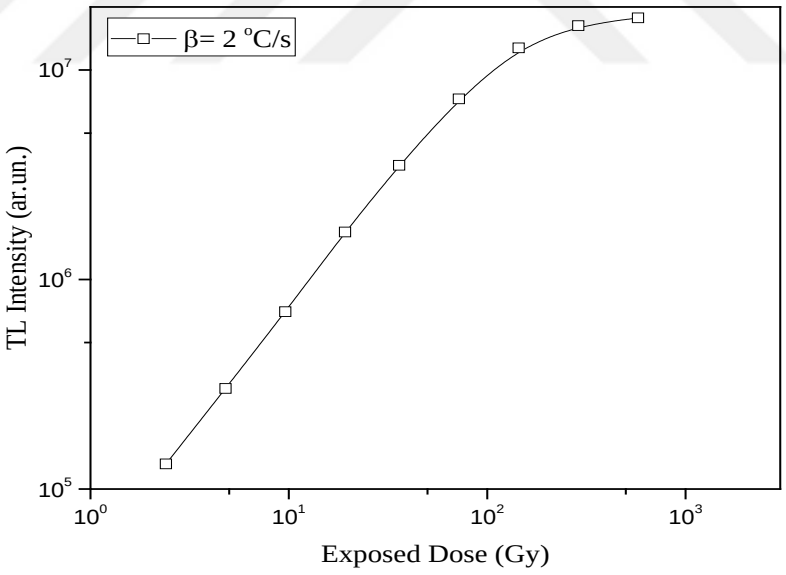

(b)

Figure 5.9. TL intensity vs exposed dose graphs of $CaMoO_4$:Eu at linear heating rates of (a) β = 1 $^oC.s^{-1}$ (b) β = 2 $^oC.s^{-1}$

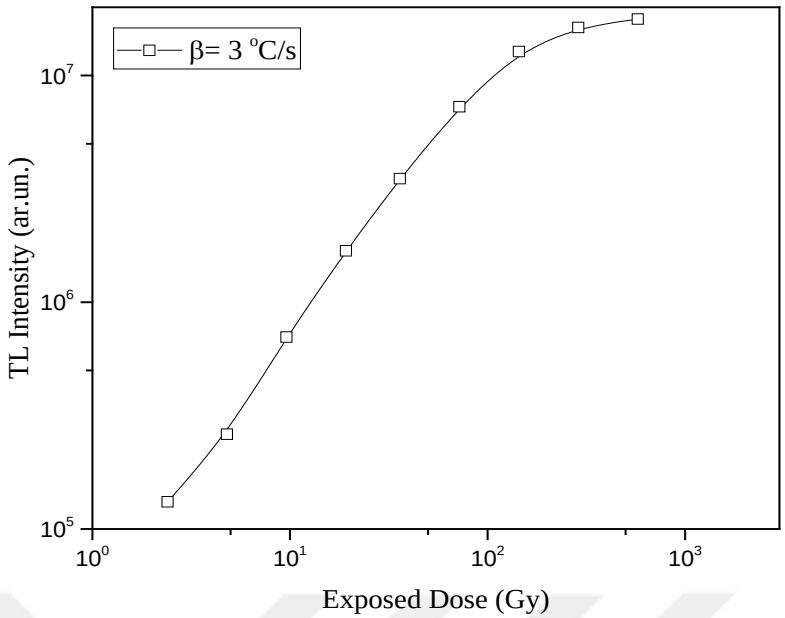

(a)

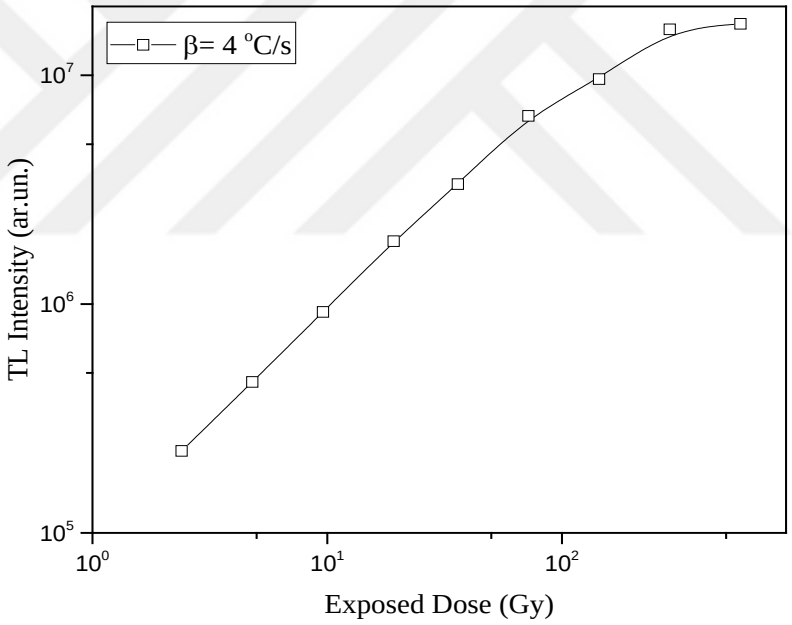

(b)

Figure 5.10. TL intensity vs exposed dose graphs of $CaMoO_4$:Eu at linear heating rates of (a) $\beta = 3\ ^{o}C.s^{-1}$ (b) $\beta = 4\ ^{o}C.s^{-1}$

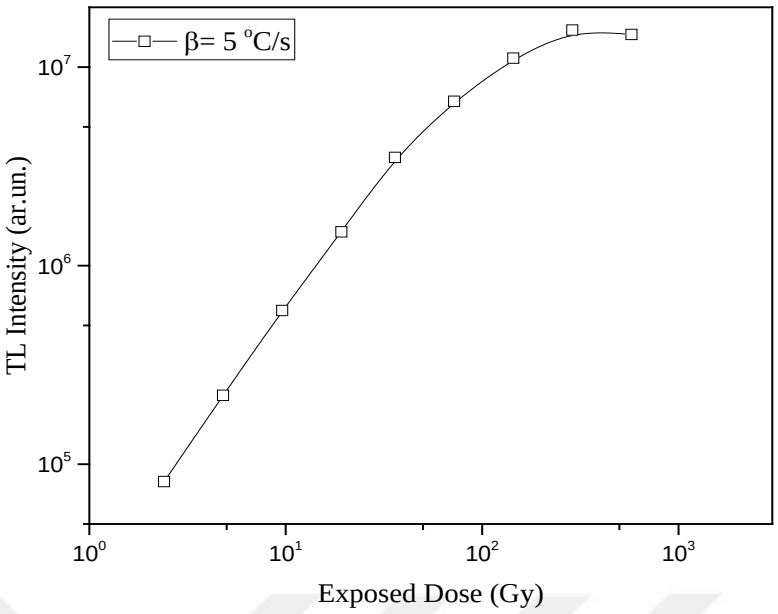

(a)

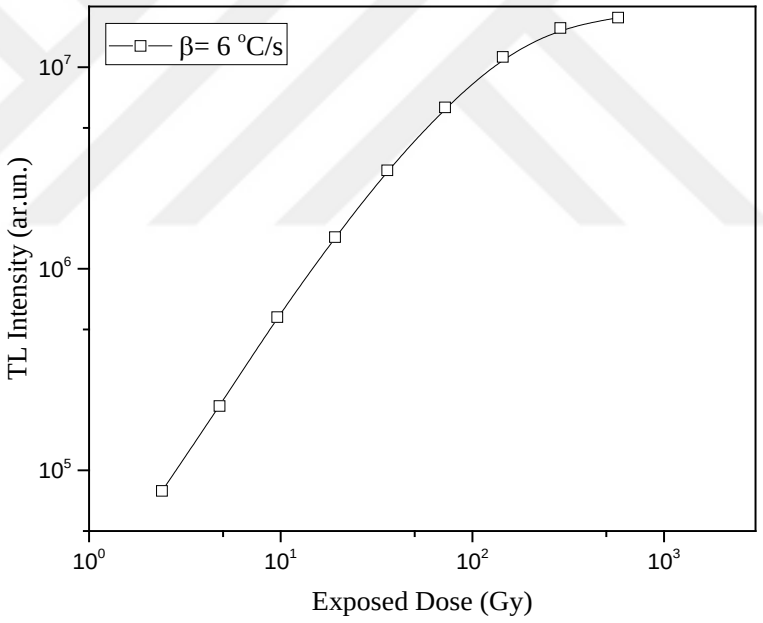

(b)

Figure 5.11. TL intensity vs exposed dose graphs of $CaMoO_4$:Eu at linear heating rates of (a) $\beta = 5\ ^oC.s^{-1}$ (b) $\beta = 6\ ^oC.s^{-1}$

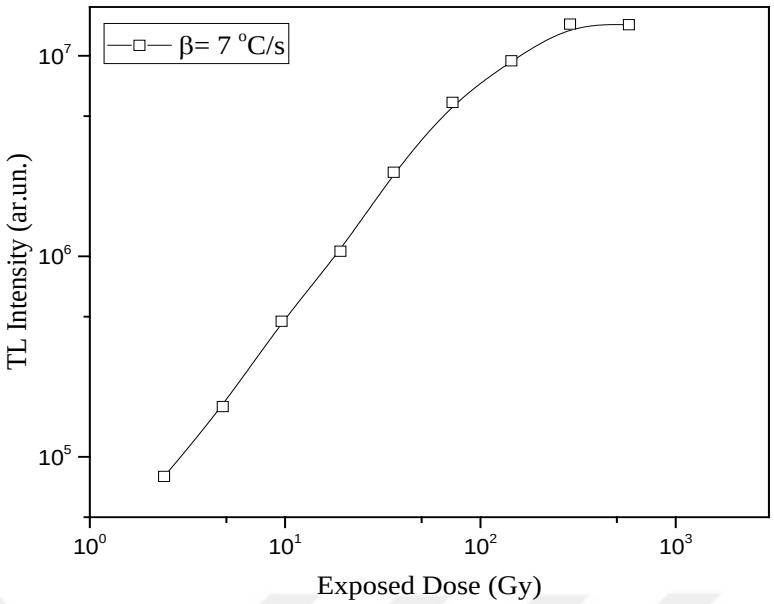

(a)

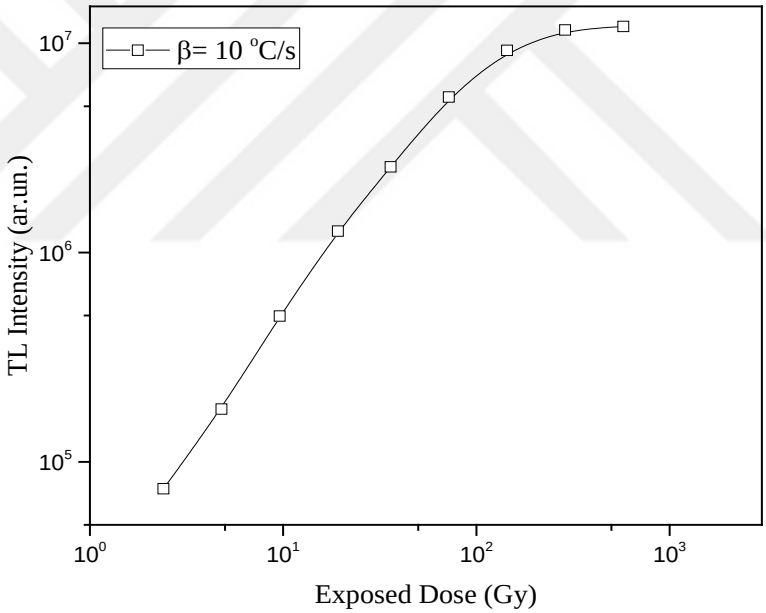

(b)

Figure 5.12. TL intensity vs exposed dose graphs of $CaMoO_4$:Eu at linear heating rates of (a) $\beta = 7\ ^oC.s^{-1}$ (b) $\beta = 10\ ^oC.s^{-1}$

After determining the dose response behaviours of the TL intensity of the main glow peak of $CaMoO_4$:Eu we have also checked the total peak area of the glow curves at different linear heating rates between 1 °C/s and 10 °C/s. Figures 5.13-5.15 shows the evaluated TL area vs exposed dose graphs.

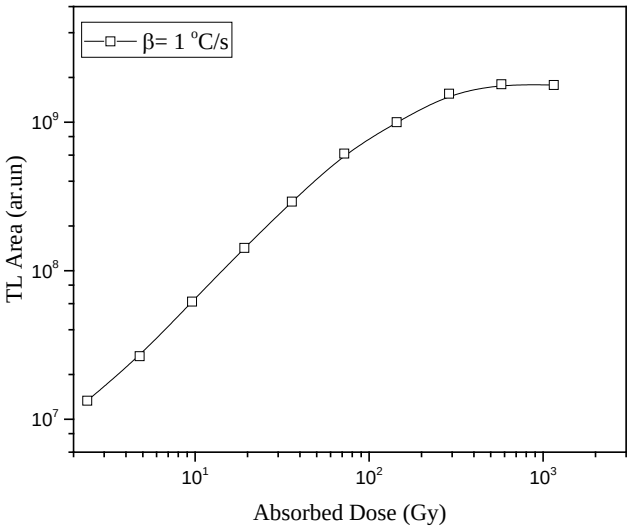

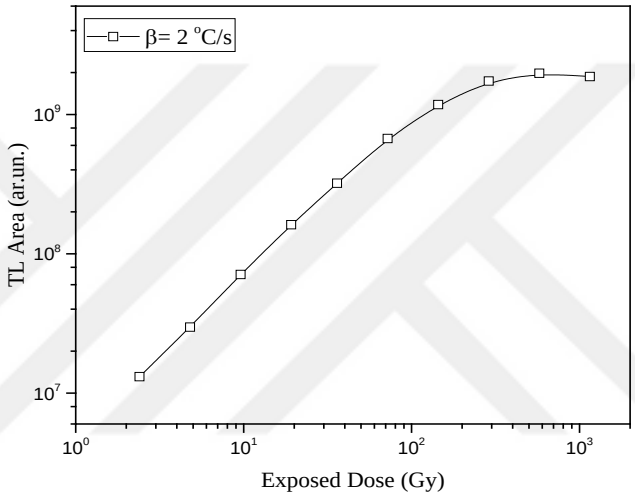

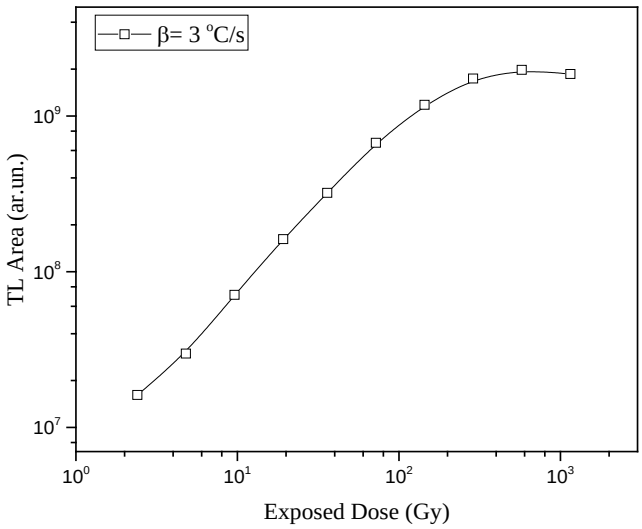

Figure 5.13. Total area vs exposed dose graphs $CaMoO_4$:Eu at linear heating rate of (a) $\beta = 1\ ^oC.s^{-1}$, (b) $\beta = 2\ ^oC.s^{-1}$ and (c) $\beta = 3\ ^oC.s^{-1}$

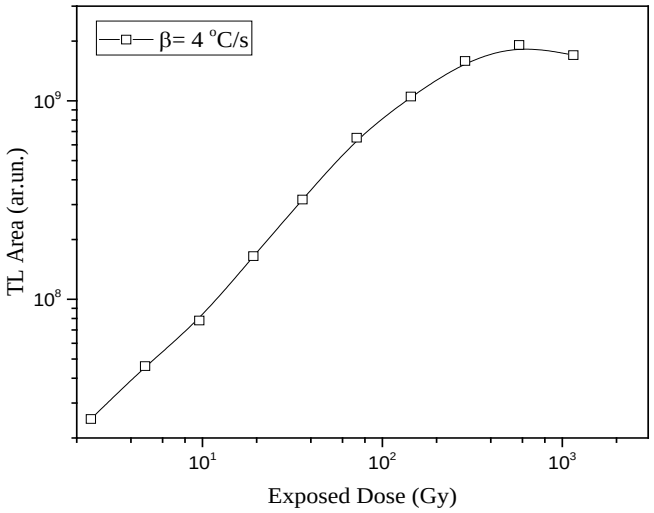

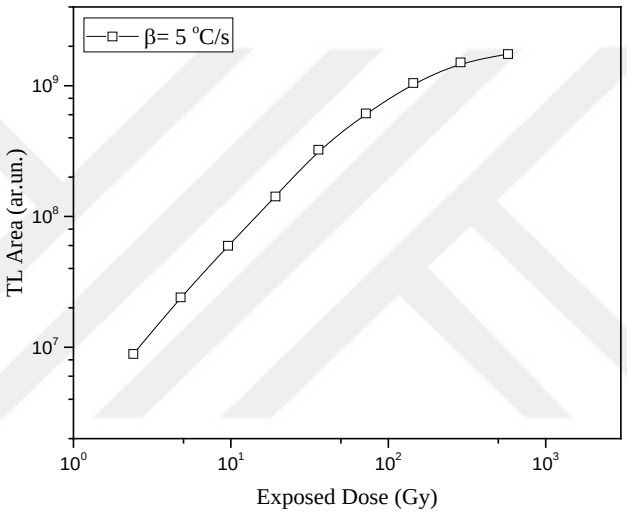

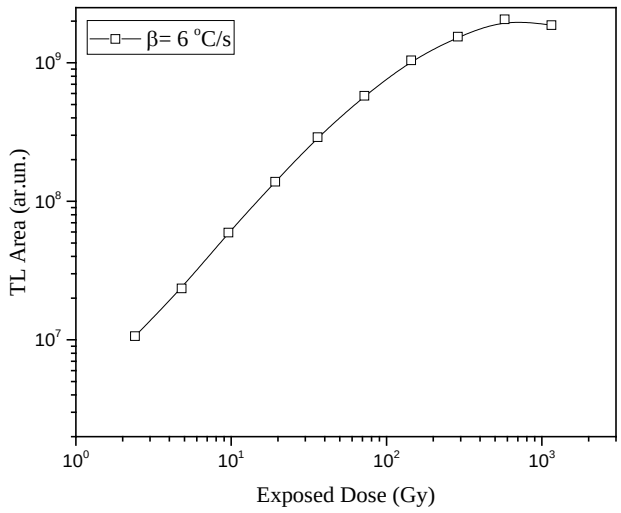

Figure 5.14. Total area vs exposed dose graphs $CaMoO_4$:Eu at linear heating rate of (a) $\beta = 4\ ^{o}C.s^{-1}$, (b) $\beta = 5\ ^{o}C.s^{-1}$ and (c) $\beta = 6\ ^{o}C.s^{-1}$

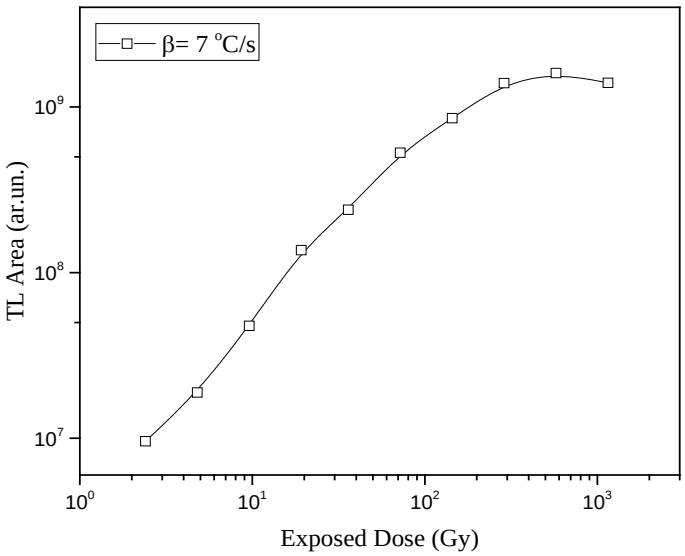

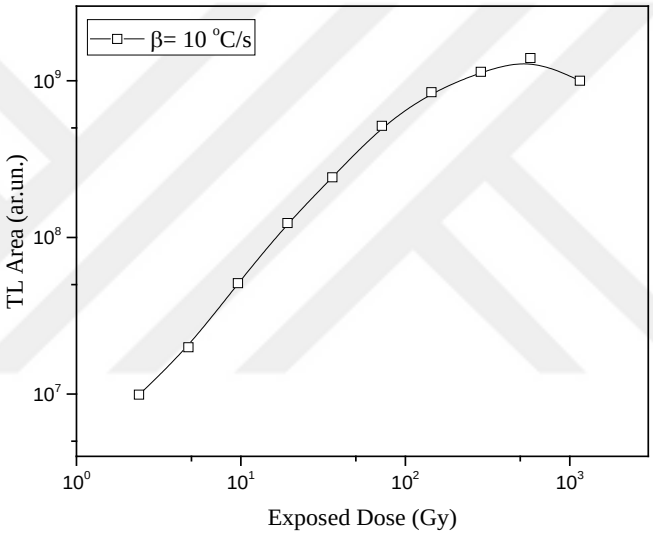

Figure 5.15. Total area vs exposed dose graphs $CaMoO_4$:Eu at linear heating rate of (a) β = 7 $^{o}C.s^{-1}$ and (b) β = 10 $^{o}C.s^{-1}$

Even figures from 5.1 to 5.15 explain the growth of the height of the peaks and the total peak area as a function of exposed dose at different linear heating rates, to best understand the dose rate behavior of the peaks the dose response function, *f(D)*, is estimated by utilizing equation (3.2**).** For the main glow peak *f(D)* of Eu doped $CaMoO_4$, namely a linear *(f(D)=1)*, pursue by a part of supralinear growth *(f(D)>1)*, progressively going into a part of sublinear growth *(f(D)<1)*. As seen from the figures from 5.16 to 5.18..

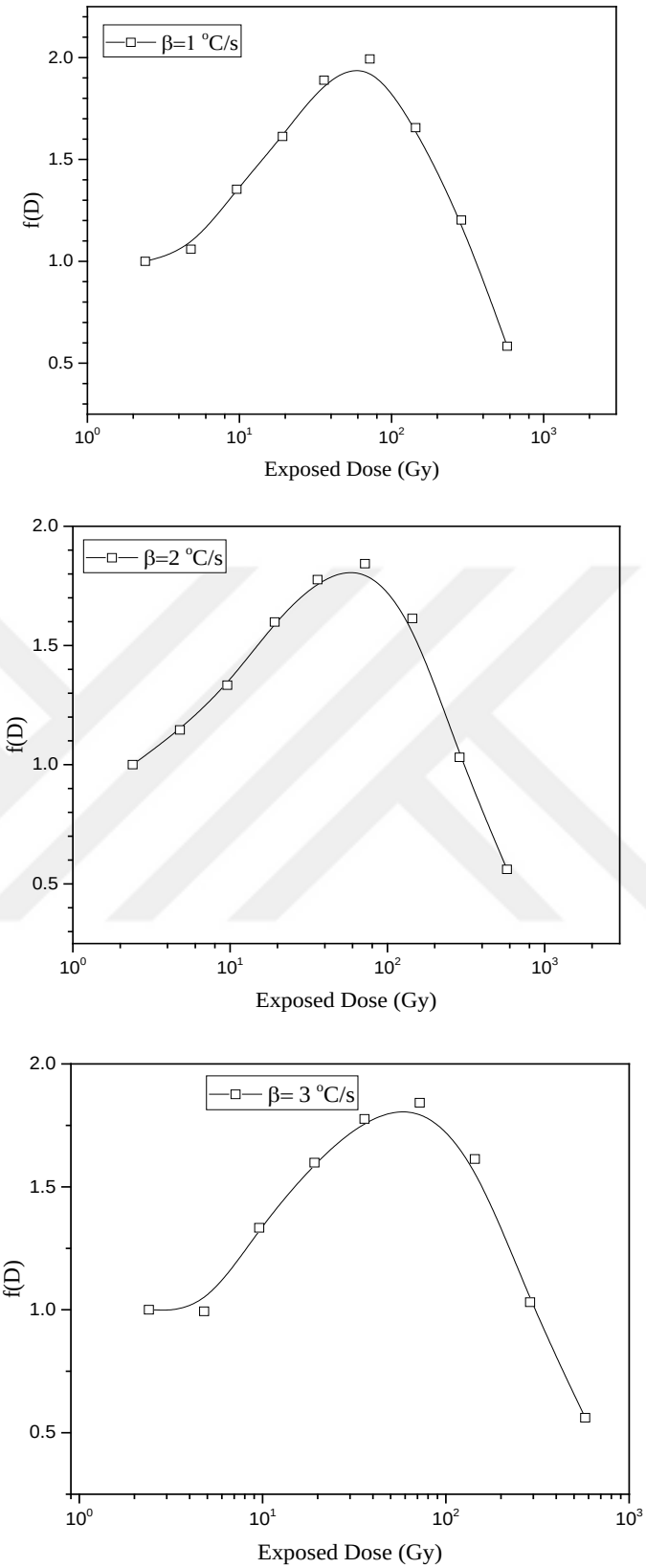

Figure 5.16. The dose response function *f(D)* vs *D* of $CaMoO_4$:Eu (β = 1 $^oC.s^{-1}$, 2 $^oC.s^{-1}$, 3 $^oC.s^{-1}$)

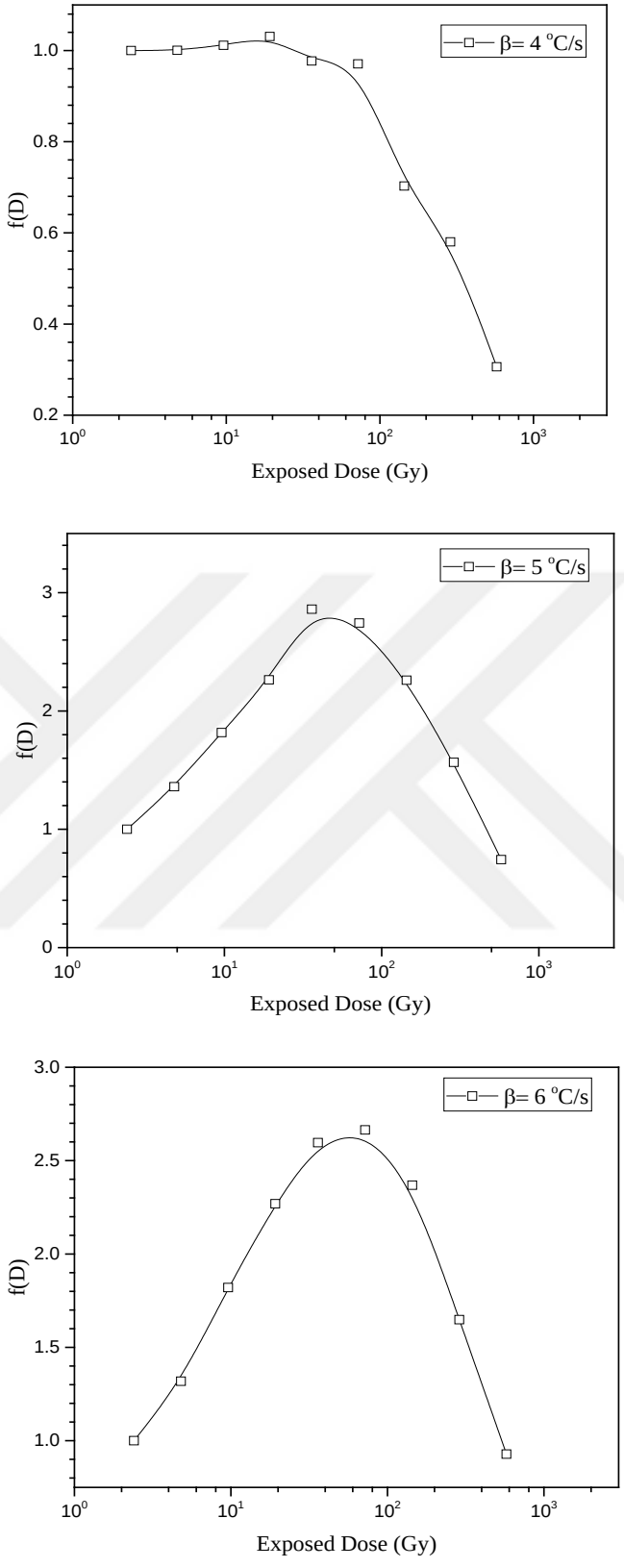

Figure 5.17. The dose response function *f(D)* vs *D* of $CaMoO_4$:Eu (β = 4 $^oC.s^{-1}$, 5 $^oC.s^{-1}$, 6 $^oC.s^{-1}$)

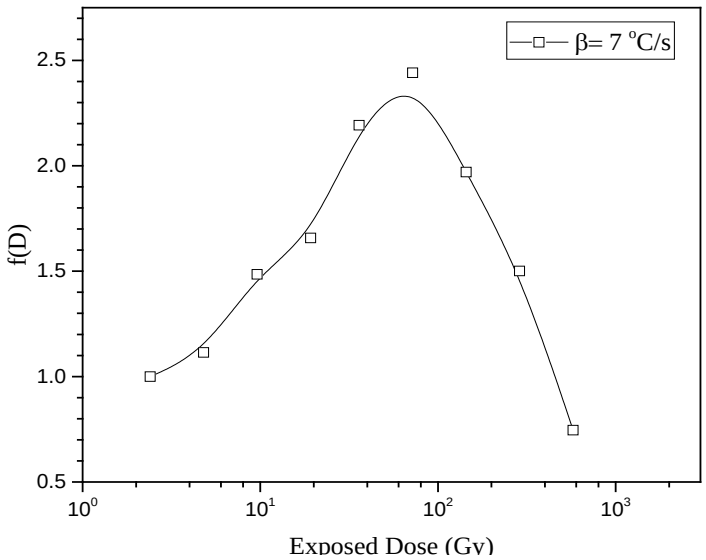

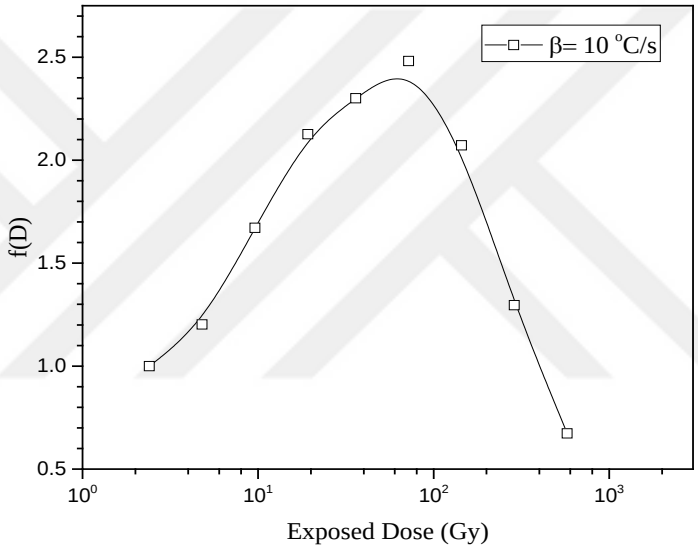

Figure 5.18. The dose response function *f(D)* vs *D* of $CaMoO_4$:Eu (β = 7 $^oC.s^{-1}$, 10 $^oC.s^{-1}$

The evaluated f(D) functions at different linear heating rates has clearly shows that the glow curve show linear *(f(D)=1)* behavior at very low doses then the curves are supralinear *(f(D)>1)* up to nearly 10^2 Gy, after this dose level the peaks saturates and goes into sublinear *(f(D)<1)* region the heating rates (β) of 1 ^{o}C/s, 2 ^{o}C/s, 3 ^{o}C/s, 5 ^{o}C/s, 6 ^{o}C/s, 7 ^{o}C/s and 10 ^{o}C/s. But the curves show very different behavior at heating rates of 4 ^{o}C/s. As seen from the figure 5.17 the peak show linear *(f(D)=1)* behavior nearly up to 100 Gy, and after this dose level the peak suddenly saturates and goes into sublinear *(f(D)<1)* region.

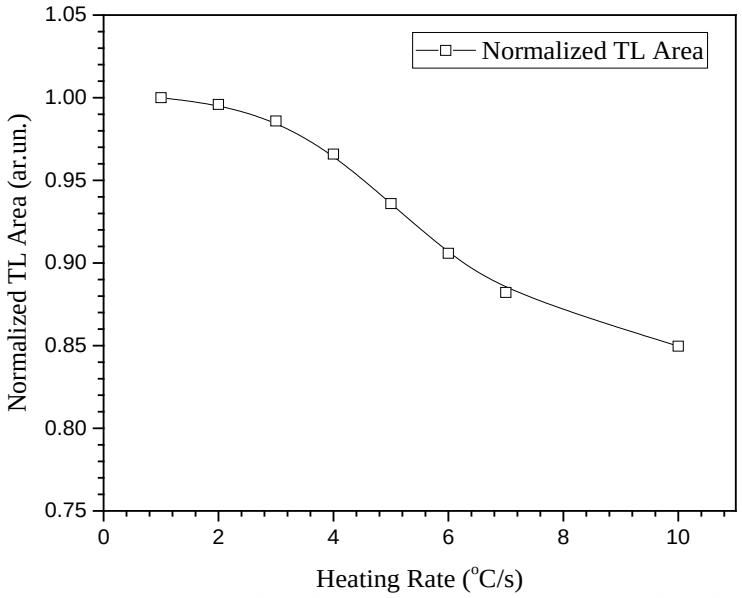

(a)

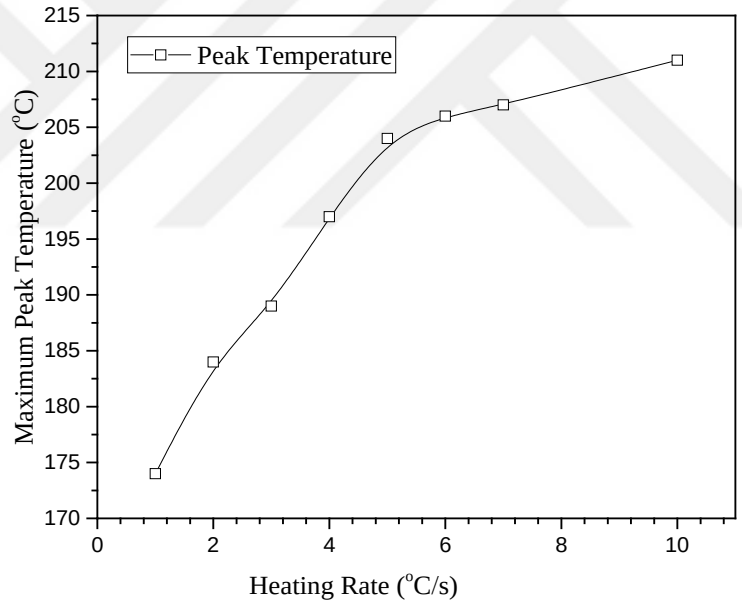

(b)

Figure 5.19. Normalized total TL peak area and the change of the peak temperature of $CaMoO_4$:Eu irradiated with ^{90}Sr-^{90}Y source at heating rates between 1 $^oC.s^{-1}$ and 10 $^oC.s^{-1}$ (D=72 Gy)

We have also evaluated the normalized total peak area and peak temperature of the main dosimetric peak of $CaMoO_4$:Eu vs heating rate. As seen from the figures 5.19a and 5.19b the normalized total peak area decreases by nearly %15 and the maximum

peak temperature of the main glow peak increases from 173 °C to 213 °C as stated in the theory.

As a last part we have also studied in this thesis the storage time effect on the intensity of the glow peaks of Eu doped $CaMoO_4$. For this experiment, the material was irradiated up to 36 Gy. The storage time experiments were performed for different time periods. The figure 5.20 shows the measured glow curves at the end of the scheduled storage periods. As shown from the figure 5.21 the total peak area of $CaMoO_4$:Eu at the end of the scheduled storage times reduced typically 40 % of its original value.

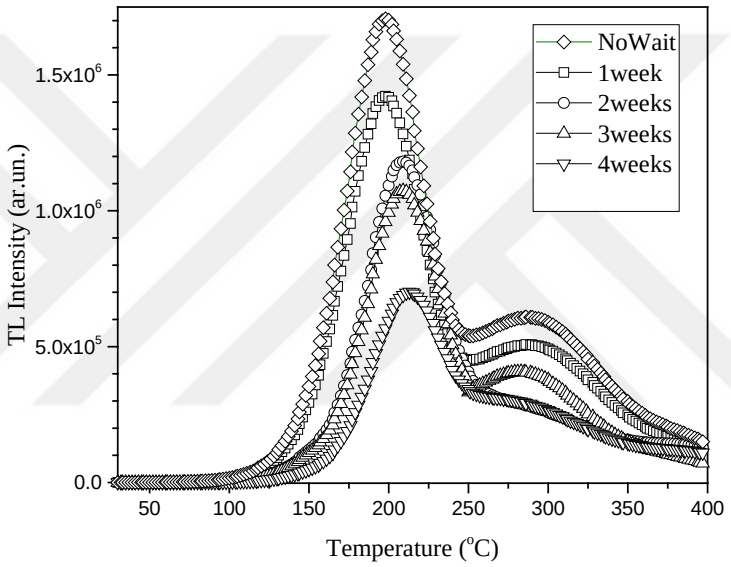

Figure 5.20. Thermoluminescence glow curves of $CaMoO_4$:Eu after various storage periods at RT after exposing to an irradiation of 36 Gy.

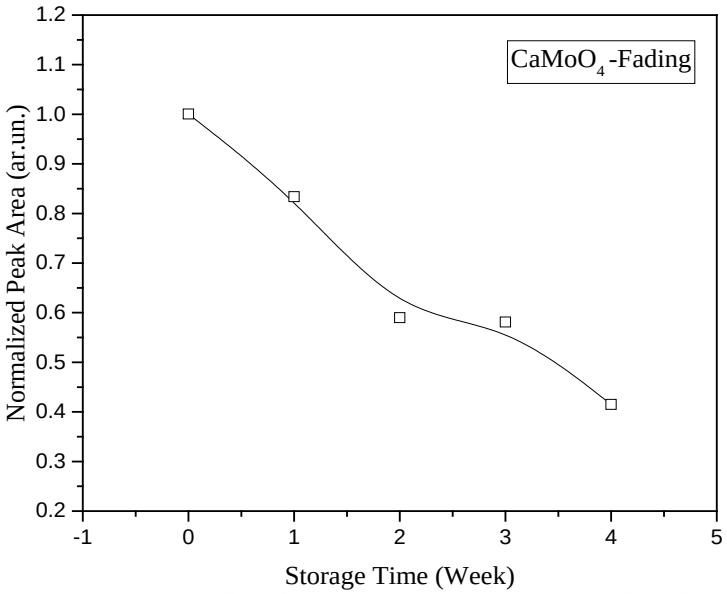

Figure 5.21. Normalized TL intensity of $CaMoO_4$:Eu after different storage times at room temperature. (β=1 $^oC.s^{-1}$ and D=36 Gy)

CHAPTER 6

CONCLUSION

In this search, we have investigated the dose response characteristics of Eu doped $CaMoO_4$ from 2.4 Gy up to 576 Gy. So as to grasp the nonlinearities in the dose dependence of this pattern, the supralinearity function, *f(D),* was estimated by utilizing equation 3.2. The dose response characteristics of the glow curves at different linear heating rates has been given in figures from 5.1 to 5.8. The curves clearly show the main features characteristic of the dose response. In general all of the peaks appear linear behavior at low doses, *f(D)=1*, pursue by a field of supralinear growth *(f(D)>1),* than progressively going into a field of sublinear evolution *(f(D)<1)* at high doses.

In this thesis we have investigated the influence of heating rate on the linearities and the TL intensities of glow peaks of Eu doped $CaMoO_4$ at various linear heating rates between 1 $^oC/s$ and 10 $^oC/s$. Our essential target is a try to understand the influence of linear heating rate on the dose response characteristics and linearity of Eu doped $CaMoO_4$ by utilizing the supralinearity index *f(D).* To have a information about dose response characteristics of the glow curves, firstly we have evaluated of the height of the peaks as a function of dose. As it is seen from the figures while the dose level is increased, the peaks show linear behavior up to a certain dose level then the peaks saturates and go into the sublinear region. After determining the dose response vs TL peak intensity graphs we have also evaluated the dose response vs total peak area and we got the same results as the previous ones. As well as the evolution of the height of the peaks and total peak areas as a function of exposed dose clarify the dose response behaviors, the dose response function, *f(D),* is also estimated by using equation 3.2 in order to better understand the dose rate behavior of the peaks. It can be concluded from the figures 5.16 - 5.18, the glow curve show linear *(f(D)=1)* behavior at very low doses then the curves are supralinear *(f(D)>1)* up to nearly 10^2 Gy, after this dose level the peaks saturates and goes into sublinear *(f(D)<1)* region the heating rates (β) of 1 $^oC/s$

, 2 ºC/s, 3 ºC/s, 5 ºC/s, 6 ºC/s, 7 ºC/s and 10 ºC/s. But the curves show very different behavior at heating rates of 4 ºC/s. As seen from the figure 5.17 the peak show linear *(f(D)=1)* behavior nearly up to 100 Gy, and after this dose level the peak suddenly saturates and goes into sublinear *(f(D)<1)* region. Nonlinearities oftentimes happen in the dose dependence of thermoluminescence (TL). These contain sublinearity, generally when there is a path to saturation in the dose dependence, as well as supralinearity, same times termed superlinearity in the literature. Several researchers in the domain have checked the influence of supralinearity /or superlinearity from two a little bit different points of view. Number one point of view has to do with the rate of change with dose of the dose dependence function. The other path is concerning more to the applications of TL in dosimetry and geological dating and archaeological, and basically has to do with the correction to be made in extrapolation in cases where supra (super) linearity occurs following an initial linear dose range, or prior to such a linear range. The influence of heating rate (β) on the glow curves can be preferable portrayed by the influence of thermal quenching. It is well known that the dosimetric characteristics of numerous TL substances are influenced by changes in location, shape and size of the glow curves due to changes in the heating rate (β). Thermal quenching was grasp to be due to the growing probability of non-radiative transitions competing with the radiative transitions. Since the growing in the heating rate resulted in a growing in the temperature of the TL glow peak, this change in temperature was held responsible for the growing in the contribution of non-radiative transitions. Then, it was derived that the glow peaks appearing at higher temperatures must display high thermal quenching than those happening at lower temperatures in any TLD material. Apart from the growing probability of non-radiative transitions at higher temperatures, the spotted influences have also been assigned to the influences of heating rate on the emigration of charge carriers freed through the TL educe. The consequences of this search appeared that, the peak temperatures of all peaks are shifted higher temperatures and the integrated peak area of the curves decreases as the heating rate increases as expected in theory. As seen from 5.1 the peak temperatures of all peaks are shifted higher temperatures when the heating rate increases as expected in theory. It is also seen from figure 5.21, the total peak area of the glow curves decreases as the heating rate increases. The total area of the glow curves were normalized at the lower heating

rate (1 °C s^{-1}) and it can be seen that the decrease in the integrated area of the peaks by about 40%.

REFERENCES

[1] Herman Cember and Thomas Eohnson (2009). Introduction To Health Physics (Fourth Edition).

[2] Chen, R. McKeever. S. (1997). Theory of Thermoluminescence and Related Phenomena. World Scientific Publishing Co. Pte. Ltd., Singapore.

[3] Mihaltsenko. G.A.(1967) Radiation physics.

[4] Savikhin. F.A.(1974) Proceedings of inst. Of physics of est. Acad. Sci.

[5] Makeovers S.W.S. 1988 Thermoluminescence of solids. Cambridge: Cambridge university press.

[6] Othman I E and Charles M.W. (1999) thermoluminescence properties of novel thin clear fused quartz dosemeters, *Radiation Protection Dosimetry*

[7] M.G.Guelev. I.T. Mischev. B.Burgkhardt and E.Piesch, (1994). *Radiation Protection Dosimetry*.51 -35.

[8] Randall, J. T., and Wilkins, M. H. F. (1945). Phosphorescence and electron traps I: The study of trap distributions. *Proceedings of Royal Society A* 184, 366-389.

[9] Pradhan, A.S. (1981). Radiation Protection Dosimetry, 1, 153.

[10] Mahesh, K., Weng, P. S., and Furetta, C. (1989). Thermoluminescence in Solids and its Applications. Ashford, Kent, England: Nuclear Technology Publishing.

[11] McKeever, SWS. Moskovitch, M., and Townsend, P.D. (1995). Thermoluminescence Dosimetry Materials: Properties and Uses. Ashford, England: Nuclear Technology Publishing.

[12] Schipper, W.J., Blasse, G., and Leblans, P. (1994). Chemistry of Materials, 6, 1784 – 1789.

[13] Furetta, C. (2003). Handbook of Thermoluminescence. Singapore: World Scientific Publishing Co. Pte. Ltd.

[14] Pekpak, E. (2009). Synthesis and Characterization of Lithium Tetraborate Doped with Metals, MS Thesis, METU, and Ankara.

[15] Schauer, D., Brodsky, A., and Sayeg, J. (2003). Handbook of Radioactivity Analysis. Second Edition. Great Britain: Academic Press.

[16] Meijerink, A., Blasse, G., and Glasbeek, M., (1990). Condensed Matter 2, *Journal of Physics*, 6303-6313.

[17] Yukihara, E.G., Gaza, R., McKeever, S.W.S., and Soares, C.G. (2004). Radiation Measurement, 38, 59-70.

[18] Randall, J. T., and Wilkins, M. H. F. (1945). Phosphorescence and electron traps II: The interpretation of long-period Phosphorescence, *Proceedings of Royal Society London* A 184, 366-389.

[19] Chen, R., Horowitz, Y.S. (1984). Thermoluminescent and Thermoluminescent Dosimetry. Boca Raton, FL: CRC Press.

[20] Kitis, G., Gomez-Ros, J.M., and Tuyn, J.W.N. (1998). Thermoluminescence glow curve deconvolution functions for first, second and general orders of kinetics, *Journal of Physics D:Applied Physics*, 31, 2636-2641.

[21] Boss, A.J.J. (2007). Theory of thermoluminescence, *Radiation measurements*, 41, 45-56. 58

[22] Hoogenboom, J.R., de Vries, W., Dielhof, J.B., Bos, A.J.J., (1988). Computerized analysis of glow curves from thermally activated processes, *Journal of Applied Physics*. 64 (6), 3193–3200.

[23] Bos, A.J.J., and Dielhof, J.B. (1991). The analysis of thermoluminescent glow curves in CaF2: Tm(TLD-300), *Radiation Protection Dosimetry*. 37 (4), 231–239.

[24] May, C.E., and Partridge, J.A. (1964). Thermoluminescence kinetics of alpha irradiated alkali halides, *Journal of Chemical Physics*, 40, 1401-1415.

[25] Gómez Ros, J.M., Kitis, G., (2002). Computerised glow curve deconvolution using general and mixed order kinetics, *Radiation Protection Dosimetry*. 101 (1–4), 47–52.

[26] Vasilis Pagonis. George Kitis and Claudio Furetta. Numerical and exercises in thermoluminescence.

[27] Lakshmanan. A.R. Madhusoodanan, U. 1998. Behaviour of CaSO4:Dy embedded Teflon discs at high annealing temperatures *Radiation Measurements*. 29 (5), 527–530.

[28] Mathur, V.K. Lewandowski. A.C. Guardala, N.A. Price. J.L., 1999. High dose measurements using thermoluminescence of CaSO4:Dy. *Radiation Measurements*. 30, 735–738.

[29] A. Halperin and R. Chen (1966), Thermoluminescence in Semiconducting Diamonds . *Physical Review Letters*. 148-839.

[30] R. Chen and S.W.S. McKeever. (1994), Characterization of Nonlinearities in the Dose dependence of Thermoluminescence. *Radiation Measurements* 23 - 667

[31] J.R.Cameron. N. Suntharalingam, and G.N. Kenney1968.*Thermoluminescent Dosimetry*. The University of Wisconsin Press

[32] Furetta, C. Prokic, M. Salamon, R. Prokic, V. and Kitis. G.(2001) *Nuclear Instruments and Methods* A, 456, 411.

[33] S.G.E. Bowman and R. Chen. (1979) Superlinear Filling of Traps in Crystals Due to Competition During Irradiation. *Radiation Protection Dosimetry*

[34] R. Chen and G. Fogel. (1993) Superlinearity in TL Revisited, *Radiation Protection Dosimetry* 47 - 23.

[35] N.Kristianpoller, R. Chen, and M. Israeli. (1974). Dose Dependence of Thermoluminescence Peaks, *Journal of Physics D: Applied Physics*. 7 1063.

[36] 9010 Optical dating system User Manuel, Dec. 1993.

[37] Yong-Song Luo, Xiao-Jun Dai, Wei-Dong Zhang, Yang Yang, Chang Q. Sun*b* and Shao-Yun Fu. (2000). Controllable synthesis and luminescent properties of novel erythrocyte-like $CaMoO_4$ hierarchical nanostructures *via* a simple surfactant-free hydrothermal route, *Dalton Trans.*,39, 2226–2231.

[38] Yonggang Wang , Junfeng Ma, Jiantao Tao, Xiaoyi Zhu, Jun Zhou, Zhongqiang Zhao , Lijin Xie , Hua Tian (2005). Low temperature synthesis of CaMoO4 nanoparticles, Ceramics International 33 (2007) 693–695

[39] Jing Liu, Kai Liu, Hongjian Gao, Yunzhao Liu, Chaoqin Yang, Zhongxin Liu. Synthesis and luminescence properties of CaMoO4: Er3+/Yb3+ nanoparticles J Mater Sci: Mater Electron (2015) 26:3380–3383

[40] Rohit Saraf, C. Shivakumara,N. Dhananjaya,Sukanti Behera, H. Nagabhushana Photoluminescence properties of Eu3+-activated CaMoO4 phosphors for WLEDs applications and its Judd–Ofelt analysis J Mater Sci (2015) 50:287–298

[41] Enrico Cavalli, Enrico Bovero and Alessandro Belletti Optical spectroscopy of CaMoO4:Dy3+ single crystals J. Phys.: Condens. Matter 14 (2002) 5221–5228